AD-A173 964 THE SPACE STATION MICROGRAVITY FACILITY(U) NAVAL RESEARCH 1/1
LAB WASHINGTON DC K W MEILER ET AL. 19 SEP 86
NRL-MR-5821

UNCLASSIFIED F/G 3/2 NL

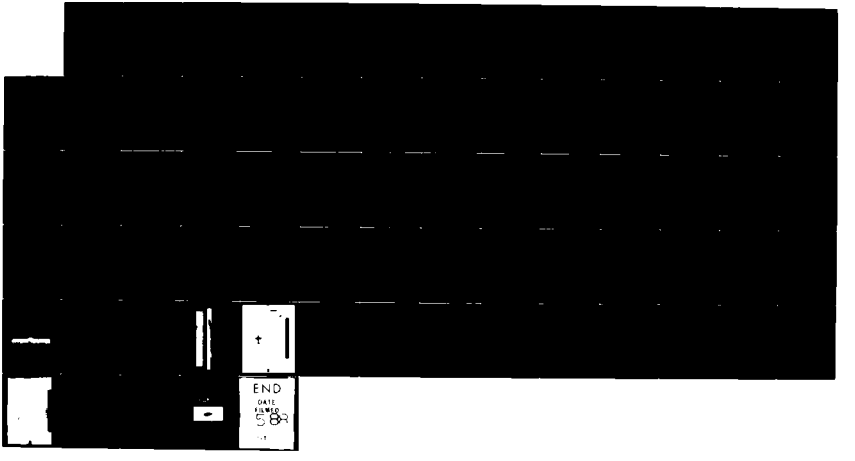

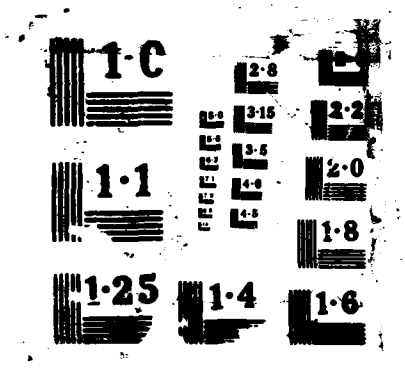
1·C
1·1
1·25
1·4
2·8
3·15
3·5
4·5
2·2
2·0
1·8
1·6

Naval Research Laboratory

Washington, DC 20375-5000 NRL Memorandum 5821 September 19, 1986

The Space Station Microwave Facility

K. W. WEILER, B. K. DENNISON, R. M. BEVILACQUA,
J. H. SPENCER, K. J. JOHNSTON, AND G. A. ANDREWS*

Radio and Infrared Astronomy Branch
E. O. Hulburt Center for Space Research

**Radar Division*

SECURITY CLASSIFICATION OF THIS PAGE

REPORT DOCUMENTATION PAGE

AD-A175 764

1a. REPORT SECURITY CLASSIFICATION UNCLASSIFIED	1b. RESTRICTIVE MARKINGS
2a. SECURITY CLASSIFICATION AUTHORITY	3. DISTRIBUTION/AVAILABILITY OF REPORT Approved for public release; distribution unlimited.
2b. DECLASSIFICATION/DOWNGRADING SCHEDULE	
4. PERFORMING ORGANIZATION REPORT NUMBER(S) NRL Memorandum Report 5821	5. MONITORING ORGANIZATION REPORT NUMBER(S)
6a. NAME OF PERFORMING ORGANIZATION Naval Research Laboratory 6b. OFFICE SYMBOL (If applicable) Code 4130	7a. NAME OF MONITORING ORGANIZATION
6c. ADDRESS (City, State, and ZIP Code) Washington, DC 20375-5000	7b. ADDRESS (City, State, and ZIP Code)
8a. NAME OF FUNDING/SPONSORING ORGANIZATION Office of Naval Research 8b. OFFICE SYMBOL (If applicable)	9. PROCUREMENT INSTRUMENT IDENTIFICATION NUMBER
8c. ADDRESS (City, State, and ZIP Code) Arlington, VA 22217	10. SOURCE OF FUNDING NUMBERS PROGRAM ELEMENT NO: 61153N; PROJECT NO: RR034; TASK NO: 06-41; WORK UNIT ACCESSION NO:

11. TITLE (Include Security Classification)
The Space Station Microwave Facility

12. PERSONAL AUTHOR(S) Weiler, K. W., Dennison, B. K., Bevilacqua, R. M., Spencer, J. H., Johnston, K. J., and Andrews, G. A.

13a. TYPE OF REPORT	13b. TIME COVERED	14. DATE OF REPORT (Year, Month, Day)	15. PAGE COUNT
Interim	FROM _____ TO _____	1986 September 19	74

16. SUPPLEMENTARY NOTATION

17. COSATI CODES		
FIELD	GROUP	SUB-GROUP

18. SUBJECT TERMS (Continue on reverse if necessary and identify by block number)
Interferometry array
Imaging astronomy
Space millimeters

19. ABSTRACT (Continue on reverse if necessary and identify by block number)

A large millimeter wavelength interferometer array is proposed for construction on the planned Space Station (The Space Station Microwave Facility—SSMF). It will have manifold applications in both basic and applied research and will be the premier instrument in the world at high radio frequencies. All weather target detection and identification, earth resource mapping, middle atmospheric studies, ionospheric research, atmospheric infrared background investigations, interplanetary communications, and high frequency radio astronomy are only a few of the areas which will be significantly advanced by the availability of such an instrument. Particularly in astronomy, the ability to do observations above the disturbing and absorbing effects of the Earth's atmosphere will allow new opportunities for exploration of all objects from the Sun, through the Solar System bodies, to the interstellar medium of the Milky Way and other galaxies, out to the most distant quasars with resolution and sensitivity equalling or exceeding all existing or planned millimeter wavelength telescopes.

20. DISTRIBUTION/AVAILABILITY OF ABSTRACT	21. ABSTRACT SECURITY CLASSIFICATION
☐ UNCLASSIFIED/UNLIMITED ☒ SAME AS RPT ☐ DTIC USERS	UNCLASSIFIED
22a. NAME OF RESPONSIBLE INDIVIDUAL K. W. Weiler	22b. TELEPHONE (Include Area Code) (202) 767-3010 22c. OFFICE SYMBOL Code 4130

DD FORM 1473, 84 MAR 83 APR edition may be used until exhausted
All other editions are obsolete

SECURITY CLASSIFICATION OF THIS PAGE

GPO U.S. Government Printing Office: 1986—607-047

CONTENTS

THE SPACE STATION MICROWAVE FACILITY

INTRODUCTION

With the increasing capability for building and maintaining large structures in space and the planned construction of a permanently manned Space Station in low Earth orbit, it is possible to consider the inclusion of a large radio telescope on the Station for a variety of basic and applied research tasks. A large microwave facility established on the Space Station will serve both as a test bed for the development and application of new technology in construction and operation techniques in space and as a source of significant new results in target detection, Earth resource sensing, atmospheric studies, deep space communications, and astronomy.

Using passive radiometry or bistatic radar, the SSMF will be able to detect reflecting objects such as ships and airplanes which stand out clearly against Earth and sea backgrounds. The positions and motions of such targets can be determined with all weather capability.

In the area of Earth sensing, the topography, composition, temperature, and ground cover of the Earth's (and sea's) surface can be studied with $\lesssim$ 100 m resolution in numerous spectral bands. The density, composition, and structure of the Earth's atmosphere can also be investigated on hectometer size scales.

For deep space communications, there is no existing facility which can communicate with spacecraft beyond the orbit of Neptune at the high bit

Manuscript approved May 14, 1986.

rates desirable for the transmission of graphic data. Even the excellent quality, superbly equipped 70 m NASA Deep Space Network (DSN) antennas and the full array of 27 25-meter antennas of the Very Large Array (VLA) near Socorro, New Mexico provide only marginal bit rate capability at these distances. For such work, however, the high gain of the SSMF at short wavelengths will more than compensate for the larger collecting area of ground based facilities and provide the possibilitity of reliable communications throughout the Solar System.

Finally, the existence of such a facility will allow detailed investigation of many areas of astronomy including Solar System, galactic, and extragalactic sources. The chemistry and physics of giant molecular clouds, the composition and dynamics of the interstellar medium, and the processes of star formation can all be probed in far greater detail than is presently possible. From the powerful non-thermal processes in active galactic nuclei and quasars, to the dynamics of external galaxies, to the surfaces and atmospheres of the near, cold Solar System bodies, to the activity on the surface of the Sun many areas can be researched in new wavelength ranges.

These represent only a few of the disciplines where the SSMF will make a significant improvement over present and planned capabilities. Obviously, with such a major increment in instrumental power, many other areas of science and technology will be favorably affected and the possibility for unexpected new discoveries is great.

Technical Specification. To represent a significant advance over current capability and to meet the needs of the several important areas of research and application, the general requirements of the Space Station Microwave Facility (SSMF) are:

1) a large total collecting area ($\sim 10^3$ m^2),

2) a broad frequency coverage ($\nu \lesssim 10$ GHz to $\nu \gtrsim 300$ GHz),

3) a wide field of view (on Earth: $\gtrsim 10$ km at 10 GHz; on sky: $\sim 1'$ at 300 GHz),

4) a small pixel size (on Earth: $\lesssim 100$ m at 10 GHz; on sky: $\sim 1''$ at 300 GHz),

5) a broad survey capability, and

6) a flexibility of operation and application.

In order to satisfy these somewhat conflicting goals and to obtain a powerful yet flexible instrument without requiring the construction of extremely large individual structures in space, an interferometric array of 30 small antennas ("dishes") each 5 m in diameter to be arranged in a 3-arm "T" configuration with individual arm lengths of 100 m is proposed. This is shown schematically in Figure 1 where it is assumed that the stem of the "T" is along the vertical axis of the Space Station aligned with the gravity gradient, and the cross on the "T" is perpendicular to both the vertical arm and to the orbital plane. Additionally, to give high brightness sensitivity for a broad survey mode, a "single" telescope consisting of 7 dishes, each 5 m in diameter, on a single steerable mount is included in the center of the array (Figure 1). All dishes of the array are fully steerable and, in order to make optimum use of the available collecting area and to provide a large field of view, each is equipped with multiple feed horns. [A staggered array of 5 feed horns (see the resulting beam pattern projected onto the surface of the Eartn for downlooking applications in Figure 2) is considered here.] Although 5 m dishes would be usable at frequencies as low as ~ 300 MHz (wavelength 1 m) and available technology will probably permit the construction of 5 m dishes which are usable at frequencies as high as 1.5 THz (150 μm), we will not consider

applications below 10 GHz (wavelength 3 cm) or above 1 THz (300 μm). We assume that a bandwidth of 1 GHz is achievable at all observing frequencies of interest and that currently available (or almost available) low receiver noise temperatures can be maintained in space. Additionally, full polarization capability will be incorporated into the SSMF for its application to both astronomical and Earth sensing problems. These parameters for the SSMF are listed in Table 1.

With the values assumed in Table 1, the various observational capabilities of the SSMF can be calculated and are listed in Table 2. Examination of Table 2 shows that the SSMF will be an instrument of unprecedented power. It will provide both surveying and instantaneous imaging capability over a broad band of frequencies from the radio to the infrared with high sensitivity and resolution over a wide field of view. It will also be flexible in the use of these capabilities with several different modes of application for different observational needs.

Modes of Operation. With such a flexible instrument, there are numerous possible modes of operation suitable for various observing needs. All of these will be assumed to have full polarization and full spectral analysis capability. The two basic areas of application can be divided roughly into downlooking (Earth and atmospheric studies) or uplooking (celestial studies), and of these the latter will likely employ the fewest different types of observing modes and will therefore be discussed first.

Experience has shown that astronomical interferometers are almost always used in full interferometric mode with all available dishes applied to the study of the same object. Therefore, for astronomy the SSMF will generally use all 37 available dishes to map a field of interest to full resolution. The amount of integration time to be applied to a given field depends, of course, on the properties of the object to be studied and its

position on the sky, but, for objects near the plane of the orbit, the integration will be limited to approximately 30 minutes per orbit by Earth blockage on the one hand and by dish-to-dish shadowing on the other. Obviously, if more integration time is needed, observations from many orbits can be added for better sensitivity. Because the cross arm of the "T" array will be maintained perpendicular to the orbital plane of the Space Station, those celestial objects whose line of sight is nearly in the plane of the orbit can have quick "snapshot" images made while those lying in directions nearly perpendicular to the plane of the orbit will have to use rotation synthesis techniques over a large part of an orbit (assuming that the Space Station is gravity gradient stabilized with its major axis lying along a radius to the Earth's center) to obtain sufficient baseline rotation for good imaging. For surveying larger areas, the SSMF will have at least 5 feed horns per antenna providing 5 simultaneous synthesis fields on the sky. Additionally, the SSMF is designed with a central antenna consisting of 7 of the 5 m dishes on a single mount (the 7-shooter) to provide a large collecting area for quickly surveying broad areas of the sky with the relatively limited resolution needed for studying large interstellar complexes. Although the other modes of operation discussed below will also be available for astronomical observations, they are not expected to be commonly used.

For downlooking, the situation is more complicated by constraints from the relatively close horizon, by the fast motion of the Space Station relative to the areas to be studied, and by the wide variety of needs for fields of view, low and high resolutions, and sensitivities. The basic constraint on downlooking is that straight down (nadir angle = 0°; the nadir angle is that measured between the radius to the Earth's center and the angle of viewing) is not normally useful (all dishes along the vertical axis of the Space Station will shadow one another) and straight out along

the tangent to the orbit (nadir angle = 90°) misses all objects on the Earth's surface or in its atmosphere. (Some types of space based targets may still be of interest at these larger nadir angles, however.) Thus, most observations will be made at intermediate angles which we will take to be ∿45° for an incidence angle on the Earth's surface of ∿50°. Fortunately, it turns out that incidence angles close to this value are also optimum for using the full polarization capability of the SSMF to study surface properties.

Downlooking at such an angle, there are a number of options for employing the available antennas to fulfill different sensitivity, survey area, and resolution needs. These consist of several configuration modes (CM) and a like number of operation modes (OM).

CM1. The simplest configuration mode conceptually is that of many single dish, total power observations in which each of the 30 antennas in the SSMF is used independently, with its 5 independent feeds, as 5 total power radiometers. (Similarly, the 7-shooter can be used as 5 higher sensitivity total power radiometers for some types of observations.) This mode of operation provides the largest survey area (150 separate fields of view), but the lowest sensitivity and resolution.

CM2. A second possible configuration mode is to electronically split the SSMF into several sub-arrays, each operating like a separate array telescope. This mode provides better resolution and sensitivity than CM1, but with a smaller instantaneous survey area and with generally cumbersome image response patterns (synthesized beams). Configuration Modes 1 and 3 are obviously the two limiting cases for the use of sub-arrays.

CM3. The third possible configuration mode is to use all dishes of the SSMF in full interferometric operation for maximum sensitivity and resolution with high quality imaging capability. This configuration mode, of course, provides the full resolution, sensitivity, and imaging capability of the SSMF.

For each of these configuration modes (CM), there are a number of operation modes (CM) which can be employed:

OM1. the beams formed by the SSMF can be allowed to scan the Earth's surface parallel to the track of the Space Station at its 7.5 km s^{-1} orbital rate -- the "pushbroom" mode;

OM2. the beams can concentrate on a single area of the Earth's surface for the maximum length of time permitted by the physical constraints of the dish mounts, the Space Station's horizon, and the increasing path length through the atmosphere -- the "tracking" mode; and

OM3. the beams can be raster-scanned along and/or perpendicular to the Space Station's orbit to study either very large areas (larger than the pushbroom mode) very rapidly or to study intermediate sized areas (smaller than the pushbroom mode but larger than the tracking mode) with better sensitivity -- the "rastering" mode.

Each of these configuration and operation modes has its own advantages and disadvantages and its own particular uses. These are described in the following sections.

APPLICATIONS

Target Detection - Passive Radiometry. The SSMF will be an outstanding instrument for the detection, identification, and tracking of targets on the Earth's surface and in its atmosphere. Using passive radiometry, the instrument will be able to detect reflecting targets by their contrast with the "warm" Earth or sea background or absorbing targets by their intrinsic blackbody radio emission.

Metallic targets on or near the Earth's surface such as ships at sea or low flying aircraft over land or sea (high flying aircraft are, in fact, even more easily detectable by the SSMF) can be characterized as reflectors of all radiation incident from above (from the atmosphere) and blockers of all radiation incident from below (from the Earth's or sea's surface). The SSMF detects the contrast between the relatively little atmospheric radiation reflected upward by the target and the relatively large amount of background radiation blocked so that the target appears as a "cold" object on a "warm" background (Figure 3). Since both the atmosphere and the background change their emission (and absorption) characteristics with frequency, the contrast between a reflecting target and a sea or land background changes with observing wavelength. This is illustrated in Figure 4 (Hollinger, 1985) which shows the apparent brightness temperature difference (ΔT_b) between a reflecting target and a land or sea background as a function of observing frequency. As is evident from Figure 4, only frequencies $\nu \lesssim 50$ GHz and $70 \lesssim \nu(\text{GHz}) \lesssim 110$ are satisfactory, with the lower frequencies preferable. This apparent temperature contrast between the direct and reflected radiation after passing through the atmosphere must then be detected in comparison with the random noise output of the SSMF non-zero system temperatures. (The system temperature is equal to the intrinsic receiver noise plus the received ocean and atmospheric background radiation.)

Figure 4 illustrates the available contrast for good weather conditions through a standard atmosphere. However, conditions of clouds, high humidity, and rain all affect the system performance through increased absorption of the background radiation, increased emission from the atmosphere and, correspondingly, its reflected component, and increased system temperature of the SSMF. The combination of these effects is shown in Table 3 as the ratio, R, of the reflecting target to background sea brightness temperature difference ΔT_b to the SSMF system temperature T_{sys} ($R \equiv \Delta T_b / T_{sys}$) (excluding beam dilution effects) for a number of weather conditions and possible observing frequencies. A value of $|R| \lesssim 0.1$ indicates that detection becomes difficult to impossible. Examination of Table 3 shows, as expected, that under most conditions the contrast of target to sea is negative ($R < 0$; i.e., the target is "cooler"). Also apparent is that 10 GHz is an all-weather surveillance frequency where detectable contrast is obtained even under severe weather conditions of heavy rain and high humidity. At 35 GHz heavy clouds and rain severly limit the surveillance capability of the SSMF while 90 GHz is essentially a clear weather operational frequency.

Because the Space Station will be gravity gradient stabilized with its major axis aligned along a radius to the Earth's center, nadir angles for downlooking will be restricted to the range of $\sim 30°$ to $\sim 60°$. These limits are set by the angles at which the 5 m antennas along arm A (see Figure 1) of the SSMF begin to shadow one another and the angles at which projection effects and atmospheric losses become important. As a compromise between these limitations, a nadir angle of 45°, resulting in an incidence angle at the Earth's surface of 50°, has been chosen to provide optimal conditions for information retrieval both from the total intensity and linear polarization information available. The variations in brightness temperature with viewing (incidence) angle and polarization are illustrated

in Figure 5 (Hollinger, 1985).

In addition to direct detection of metallic, reflecting ships, the SSMF can detect the wakes of any vessels, independent of their composition, which are moving across the sea's surface. In contrast to "cold" metal, wakes appear "warm" against the surrounding sea at microwave frequencies. Wakes also provide information on spe nd direction of travel. Since the wake area greatly exceeds that of the ship itself, searching for wakes by scanning the SSMF at high speed can yield rapid localization of possible targets for more detailed synthesis with the SSMF of target morphology and trajectory. An example of observations taken at 90 GHz from an aircraft over a harbor is given in Figure 6 (Hollinger, 1985). The system used to produce Figure 6 has comparable resolution to that of the SSMF, and illustrates the power of this surveillance technique. The land profiles, a number of ships at anchor, and a large wake created by a ship in motion are all clearly visible.

Metallic, reflecting aircraft flying near the sea's surface have the same detectability as a ship of similar size (although leaving no detectable wake, of course). This is illustrated in Figure 7 (Hollinger, 1985) where 90 GHz observations from above clearly show the outline of a lower flying aircraft against a sea background. High flying aircraft are even more easily detected since the reduction in both atmospheric absorption and reflected atmospheric emission greatly enhances the available detection contrast.

It should be noted that, were a target to be covered with microwave absorbing material to reduce its visibility to radar, it would become a high temperature ($\sim$300 K) black body radiator for the passive radiometry of the SSMF, standing out strongly in contrast to the now relatively "cool" sea background emission (or the "cold" background of space). The detectability (ΔT_b) of several types of targets under reasonably poor

observing conditions (20° C surface temperature, light rain, and 100% relative humidity) are illustrated in Figure 8.

Target Detection - Bistatic Radar. The SSMF will also be outstanding for experiments with bistatic radar target detection and imaging from space. Such experiments can use ground based transmitters, either specially tasked or transmitters of opportunity, to illuminate targets or land/sea areas for detection and imaging. Likewise, airborne or space based transmitters such as SIR-X might be used. The large aperture of the SSMF will make such experiments practical for a large variety of transmitters, and measurements over a wide range of bistatic angles will be very useful in evaluating radar performance theory. The SSMF can also be used to yield large area bistatic clutter measurements which cannot otherwise be obtained.

Target Detection - Summary. To summarize, for target detection on the Earth's surface or in its atmosphere, the SSMF will be able to survey large areas with high sensitivity (for small ΔT_b contrast detection) and resolution (for target position, motion, and morphology determination). Additionally, its frequency flexibility will allow the choice of higher resolution imaging of smaller areas under good weather conditions at higher frequencies (e.g., 90 GHz) or lower (but still good) resolution surveying of larger areas under all weather conditions at lower frequencies (e.g., 10 GHz). The various system parameters for the SSMF at different possible surveillance frequencies are summarized in Table 4.

Table 4, Column 1 lists the 3 frequencies which are likely to be of most interest for surveillance. At each of these frequencies, the size of the field of view to half power for a single primary beam of the SSMF is given in Column 2, and in Column 3 the maximum width of the pushbroom formed by the 5 primary beams is given. (A possible arrangement of the 5

primary beams in the SSMF pushbroom is illustrated in Figure 2.) Table 4, Column 4 gives the resolution of the full SSMF operating 37 dishes in full interferometric mode (CM3) and Column 5, top half, lists the survey rate for the 5 beam swath aligned perpendicular to the orbit and sweeping at the orbital rate of the Space Station of 7.5 km s^{-1} (pushbroom mode, OM1). These values determine the available integration time in this pushbroom mode (Table 4, top half, Column 6) and, correspondingly, the sensitivity to targets (temperature contrast ΔT_b) under two very different sets of weather conditions (Table 4, top half, Columns 7 and 8). In the tracking mode (OM2) of observation, the survey area is much smaller (Table 4, bottom half, Column 5), but the integration time is much longer at $\sim$60 seconds (the approximate time for the nadir angle to change from 60° to 30°; Table 4, bottom half, Column 6) and the target sensitivities are better (Table 4, bottom half, Columns 7 and 8).

Even with its short integration time and wide search area, the pushbroom mode of observation provides an effective all weather surveillance capability at 10 GHz because of the great sensitivity of the SSMF. A target as small as 1400 m^2 (approximately the size of a small ship) will be easily detectable against a sea background in a single sweep. At 35 and 90 GHz, under good weather conditions and with the correspondingly smaller swath widths, target sensitivity is greater and smaller targets become detectable. At 90 GHz the SSMF is sensitive even to patrol boats and bomber sized aircraft.

Using additional configuration and/or operation modes may be advantageous under certain circumstances. For example, by splitting the SSMF electronically into separate sub-arrays (CM2), increased survey areas can be obtained at decreased sensitivity. With four independent sub-arrays at 10 GHz, a pushbroom swath width of 88 km can be obtained. Although this mode has relatively low sensitivity to ships, it is readily capable of

detecting wakes which, once detected, allow examination of the originating ships in one of the high sensitivity modes. These relations between observing frequency, swath width, number of sub-arrays, and possible targets are illustrated in Figure 9.

When rastering (OM3) with the SSFM, i.e. with the antennas scanning rapidly over the large areas of the Earth's surface visible at any instant from the Space Station (up to ∿700 km from the nadir point below Station's position), the integration times are correspondingly shorter and the sensitivity per area correspondingly lower. However, in most cases the maximum area which can be surveyed in this mode is not limited by the minimum integration time but by the maximum mechanical nodding rate of the 5 m antennas of the SSMF. This is assumed to ∿1 Hz which, for example, restricts the rastering survey area to 2×10^6 km^2 at 10 GHz, 2×10^5 km^2 at 35 GHz, and 2×10^4 km^2 at 90 GHz per orbit. These relations between survey area and detection sensitivity are illustrated for metallic, reflecting targets against a sea background in Figure 10. Clearly, very large areas can be raster scanned with high sensitivity in a single orbital pass. For example, the SSMF at 10 GHz can detect all ships which are destroyer sized and larger within a 10^4 km^2 area per orbit while the 35 GHz system (under good weather conditions), will be sensitive to frigate sized ships within a comparable area. The SSMF will be able to detect patrol craft and bomber sized aircraft over somewhat more restricted areas.

Earth Sensing. Table 5 lists a number of phenomena on the Earth's surface which are known to affect its microwave brightness temperature (Ulaby, Moore, and Fung, 1981). These variations in brightness temperature (ΔT_b) occur over different size scales from many hundreds of kilometers to only a few meters in size and Table 5 indicates whether they will be most amenable to study with the single dish total power, moderate resolution mode (CM1)

of observation with the SSMF or with the full interferometric synthesis, high resolution mode (CM3) of observation. The Earth surveying capabilities of these two possible observing modes are given in Table 6.

It should be noted that the moderate resolution configuration (CM1) provides an enormous pushbroom swath due to the large number of separate antennas (30) and beams per antenna (5) available. Hence, extremely large areas of the Earth's surface can be surveyed very rapidly. This permits large scale monitoring of variations in gross surface properties. Most, if not all of the phenomena listed in Table 5 will show large scale temporal changes of considerable interest. The full interferometric, high resolution mode (CM3), on the other hand, provides remarkably fine detail for surveying small scale features on the Earth's surface and will permit high resolution comparison of microwave images with infrared and optical pictures.

The 3σ brightness temperature sensitivities (ΔT_b) given in Table 6 show that the SSMF will have excellent sensitivity to many of the Earth's surface phenomena such as those listed in Table 5 (Hollinger and Lo, 1984; Lintz and Simonett, 1976; Pampaloni and Paloscia, 1985; Ulaby, Moore, and Fung, 1982). Also, the availability of full polarization will provide additional information on the properties of regular surface features such as sea roughness (see, e.g., Figure 5). Clearly, the SSMF will constitute a major advance in Earth sensing with its capability for making rapid, high resolution, high sensitivity microwave emissivity and polarization measurements of large areas.

Atmospheric and Ionospheric Studies. For atmospheric studies, the SSMF can be used as a line spectrometer in a limb scanning mode to make composition measurements in the middle atmosphere (15 - 100 km height). Many atmospheric constituents, some of which are already known to be important

to our understanding of atmospheric chemistry and physics, have spectral lines in the millimeter wavelength range. Observations in this range, in fact, have distinct advantages over infrared measurements, the most prevalent data available today, because the millimeter lines are much more widely spaced. This avoids the extreme complication of the infrared telluric lines which are due to many overlapping vibration-rotation transitions. Single isolated millimeter rotational lines can be easily observed and the non-LTE (non-local thermodynamic equilibrium) effects which plague infrared measurements above the stratopause (>50 km height) do not become important until much higher (>100 km).

Evidence of the importance of remote sensing at millimeter wavelengths for atmospheric studies is the rapid increase in the number of ground-based measurements during the last 10 years and the plans for space-based instruments in the near future. The Microwave Atmospheric Sounder (MAS) will be carried aboard the Space Shuttle in November 1988 and the Millimeterwave Limb Sounder (MLS) will be carried aboard the Upper Atmosphere Research Satellite (UARS) to be launched in late 1989.

The SSMF, however, will be a much more powerful instrument for atmospheric studies due to its superior sensitivity, spatial resolution, frequency coverage, spectral resolution, and flexibility of operation. Table 7 lists a number of constituents of the middle atmosphere whose investigation is important for atmospheric research and which possess rotational lines in the 10 GHz to 1 THz frequency range of the SSMF. With the capability to study these with high spatial and frequency resolution and with good signal to noise, a number of important topics can be attacked.

Ozone is a vital constituent of the middle atmosphere which shields the Earth's surface from the harmful effects of solar ultraviolet radiation. Although life as we know it could not exist without this screening layer,

the layer appears to be extremely fragile and may be becoming depleted by antropogenic effects such as the release of freons used in refrigeration and nitrogen products used for fertilization. The creation, destruction, distribution, and transport of ozone must be better understood so that, with the aid of middle atmospheric photochemical models, a prognostic capability can be achieved. Since ozone interacts photochemically with many other atmospheric species and is also controlled by dynamical processes, the distribution of these atmospheric constituents must also be measured and the atmospheric transport processes understood to obtain a comprehensive model of the abundance and global distribution of ozone.

The SSMF with its high resolution and sensitivity will contribute significantly to this goal. It will permit the distribution of ozone itself to be measured on a global basis over long time scales. Additionally, the two quantities which most critically control the ozone abundance in the mesosphere [water vapor (H_2O) and atmospheric temperature] can be measured with the SSMF and species such as ClO, the nitrogen compounds NO, NO_2, and N_2O, and HO_2 which are involved in catalytic cycles leading to the destruction of ozone in the stratosphere (15-50 km) are potentially measurable. Thus, the SSMF can furnish a nearly complete set of data to test photochemical models and to increase our understanding of ozone related processes in the middle atmosphere.

The distribution of water vapor in the middle atmosphere is also important because this molecule appears to be an excellent tracer of vertical motions. It is believed that the breaking of gravity waves near the mesopause is the predominant mechanism for the production of vertical mixing in the mesosphere and SSMF measurements will allow the detailed mapping of these processes. Combined with the temperature and pressure measurements obtainable with the SSMF, the stratospheric wind field can be determined. There is currently great interest in determining the nature of

the coupling between the stratospheric wind field and the gravity wave vertical propagation resulting from selective filtering of these waves. With the SSMF these processes can be investigated in detail.

A further area of study for the SSMF in atmospheric physics is the distribution and transport of carbon monoxide (CO). It has numerous millimeter line transitions and, because of its rather long photochemical lifetime, is an excellent tracer of large scale motions and circulation patterns in the middle atmosphere, especially above 50 km. These circulation patterns are an important mechanism for the transport of minor constituents in the atmosphere.

Above about 60 km in the atmosphere, free electron densities begin to become large enough (owing to increased photoionization of atmospheric constituents) to affect electromagnetic wave propagation. This part of the atmosphere is referred to as the ionosphere. The ionosphere is in turn divided into layers based on the mean vertical electron density profile. The D-region is located between 60 and 85 km, the E-region extends from 85 to 130 km, and the F-region is above 130 km (Brasseur and Solomon, 1984). Radio waves of frequencies $\lesssim$ 10 MHz are typically reflected in the E or F-region and attenuated in the D-region with the amount of attenuation directly proportional to the free electron density. Thus, the effectiveness of many long distance communication systems is critically dependent on the electron density distribution in the D-region, and an understanding of the temporal and spatial variability of the electron abundances in this region is of utmost importance.

In the D-region, ionization results mainly from the photoionization of NO by Lyman alpha and, to a lesser extent, ionization of O_2 by X-rays and cosmic rays. However, below about 80 km the D-region positive ion composition is dominated by heavy $H^+(H_2O)_n$ type ions, where n can be as high as 10 (Brasseur and Solomon, 1984). These heavy ions are formed from

complex reactions starting with NO^+ and O_2^+ and their density depends upon the NC, H_2C, and CI abundances and on temperature. Lack of knowledge of these parameters has led to a large uncertainty in our understanding of the chemistry of the D-region. The SSMF will be particularly important for studies of this region because it can directly measure most of the quantities needed for detailed study of the chemical processes taking place. These values will then result in a better characterization of the ion and electron densities in the D region as a function of geophysical conditions and season. This may ultimately lead to a predictive capability for these abundances and provide a more efficient and effective use of strategically important communication systems.

The measurement of atmospheric constituents in the middle atmosphere by the SSMF will also be important for space-based, infrared, strategic surveillance systems. Effective operation of these systems requires detailed knowledge of the atmospheric infrared background and of its natural variability. The major infrared-active species in the middle atmosphere are CO_2, H_2C, C_3 and, to a lesser extent, N_2C, CC, and CH_4. Unfortunately the distribution of these species is not presently known in sufficient detail to permit accurate characterization of the infrared background. The SSMF will be able to provide global, long-term, direct measurements of all of these constituents with the exception of CO_2 and CH_4. (These are linear molecules posessing no permanent dipole moment and thus no pure rotational spectrum.) However, even for these last two molecules the SSMF can provide information as well since CH_4 is mainly oxidized to produce H_2O and the photodissociation of CO_2 is the dominant source of CC in the atmosphere, both of which have suitable millimeter wavelength transitions. It seems clear, therefore, that atmospheric constituent measurements provided by SSMF will greatly improve our knowledge of the infrared background. Furthermore, these and other SSMF

measurements will produce an increased understanding of the chemistry and dynamics of these infrared-active species and possibly provide a predictive capability for the infrared background currently limiting strategic detector systems.

In summary, the SSMF is relevant to a number of the most important problems being attacked in middle atmospheric science today: ozone photochemistry, atmospheric dynamics, D-region electron abundances and chemistry, and infrared background. This broad applicability clearly places the SSMF as the most important instrument for atmospheric science yet proposed.

Deep Space Communications. The past two decades have witnessed an explosive growth in our knowledge of the Solar System, primarily through unmanned probes to other planets. Mars and Venus have been observed in great detail with both orbiters and landers and Jupiter and Saturn have been closely approached by interplanetary probes. However, the outer planets, Uranus, Neptune, and Pluto remain largely unexplored. This situation is now improving with the mission of Voyager to Uranus and Neptune, but there are severe problems of communicating with spacecraft at these distances. This is especially true since imaging is one of the most important functions of planetary probes but it requires very high data transmission rates at good signal to noise. For example, the Voyager telecommunications system (Edelson et al., 1979; Brejcha, 1980), the most advanced yet flown (see Table 8 for system parameters), was designed with a number of unique features enabling it to deliver high quality television pictures at high bit rates from Jupiter and Saturn to the 64 m Deep Space Network (DSN) antennas. These features include the use of a high frequency data link (X-band, 8.4 GHz), an on board 3.7 m antenna, and advanced coding techniques. (A signal-to-noise ratio of 1.82 was required to achieve the

0.5% or smaller bit error rate required for the transmission of images.) The result was excellent quality images at a high bit rate of 115 kb s^{-1} from Jupiter and at a lower bit rate of 44.8 kb s^{-1} from Saturn. Reference to Figure 11, however, shows that this communications system is marginal for transmissions from the outermost planets. For the January 1986 Uranus flyby, the information coding had to be reprogrammed for improved signal-to-noise and for the 1989 Neptune encounter the Very Large Array (VLA) of the National Radio Astronomy Observatory (NRAO), consisting of 27 antennas each 25 m in diameter, will be specially instrumented at 8.4 GHz to exploit its 4 times greater collecting area.

Future missions to the outer planets will require the highest possible data rates for their imaging systems while the options available to achieve substantial increases in such capability are very limited. Further reduction in receiver noise temperatures and the use of more sophisticated coding techniques are both approaching fundamental limitations. Increasing the available collecting area of the receiving antennas necessarily involves the construction of large and expensive facilities with collecting areas at least several times greater than the >13,000 m^2 of the VLA. Deploying significantly larger antennas on future spacecraft presently involves considerable engineering difficulties. Onboard recording of images for delayed, slow transmission after the planetary encounter may be useful for fly-bys, but limits the effective rate at which an orbiter can return information. Finally, available spacecraft transmitting power is severely limited by thermal load requirements.

The use of higher frequencies, resulting in much higher antenna gains, provides an attractive and reasonable solution. However, for ground-based antennas the use of shorter wavelengths increases the difficulties of attenuation and emission in the Earth's atmosphere. Even at 8.4 GHz the atmospheric limitation is potentially serious, since the system temperature

at any of the DSN stations can increase by a factor of >10 during heavy rain (Edelson et al., 1979). Hence, future advances in interplanetary telecommunications must involve high frequency receiving antennas with large collecting area in space.

The SSMF will be a major advance in this area. It will not be limited by the Earth's atmosphere and will be able to operate at frequencies >100 GHz where the high antenna gains more than offset the normally larger collecting areas (and possibly lower system temperatures) of ground-based antennas. The result is at least an order-of-magnitude increase in signal-to-noise for the SSMF over the DSN antennas. The performance of the SSMF depicted in Figure 11 shows clearly that such a system will provide the sensitivity needed for exploration to the outer reaches of the Solar System.

Astronomy. The design of a large millimeter wave radio telescope has been the topic of detailed discussion within the astronomical community since it became clear in 1983 that the planned 25 m millimeter telescope would not be built. These discussions have resulted in the outlining of a pressing need for an instrument with a total collecting area of $\sim$1000 m^2, a resolution of $\sim$1", and an ability to work at frequencies >300 GHz (wavelength <1 mm) (see Barrett, et al. 1983). With its planned collecting area of 726 m^2, its resolution at 300 GHz of $\sim$1", and its potentiality of working efficiently at both sub-millimeter and millimeter wavelengths, the SSMF will provide this ability. The capabilities of the SSMF, both the properties of the full array and of the central survey "7-shooter" element, are listed in Table 2. As is apparent from Table 2 the SSMF will provide excellent resolution, frequency coverage, and field of view. Its sensitivity to unresolved sources is outstanding in the full synthesis mode of operation [0.7 mJy (1σ) for a 30 minute integration; Table 2] and the

brightness temperature sensitivity of the central survey 7-shooter is excellent [0.43 mK (1σ) for a 30 minute integration; Table 2]. Additionally, being space based, the SSMF will not suffer from the many atmospheric limitations imposed on ground based telescopes. Figure 12 (JPL, 1985) illustrates how severe the atmospheric limitations are, even from the best known ground based site at 4,200 m altitude on the top of Mauna Kea in Hawaii. As is apparent from Figure 12, even under good conditions and in such an outstanding location, observations suffer some degradation at 300 GHz and severe degradation between 300 to 500 GHz. At frequencies above 500 GHz, ground based observations are essentially impossible because of the atmospheric absorption. The SSMF, on the other hand, will be able to work throughout the "mm-IR gap" in observations of the electromagnetic spectrum.

A comparison of the properties of the SSMF with those of other existing or planned millimeter-submillimeter wavelength telescopes is given in Figures 13 and 14. Figure 13 shows the resolution of all telescopes as a function of frequency (bottom scale) and wavelength (top scale) with better resolution at the top and poorer resolution at the bottom. As can be seen, the SSMF in the full array mode of operation has resolution approaching that of any of the existing or planned ground based interferometers [California Institute of Technology interferometer (11); University of California interferometer (12); German-French interferometer (IRAM) (13); and Nobeyama, Japan interferometer (14)] and, because it is above the atmosphere, the ability to work well even at submillimeter wavelengths. (Most telescopes have an operational upper frequency limit of $\sim$300 GHz due to their mechanical surface irregularities and even those with sufficiently accurate surfaces are limited to frequencies $<$500 GHz by the atmosphere, as has been discussed above.) It is also apparent from Figure 13 that the 7-shooter of the SSMF will be one of the most powerful "single dish" high

frequency telescopes in existence, even at frequencies transmitted by the atmosphere. It will be without peer at the highest frequencies.

Figure 14 shows, in a manner similar to Figure 13, comparison of the SSMF with existing or planned millimeter-submillimeter telescopes in terms of collecting area ($\sim$ sensitivity) with larger collecting areas at the top and smaller collecting areas at the bottom. [Since sensitivity is a function of both collecting area and antenna efficiency (as well as receiver noise temperature, etc.), since the antenna efficiency changes strongly with frequency when the dish begins to reach its upper frequency limit, and since the efficiency curve is usually not well known for most high frequency instruments, we have not attempted to display instrument sensitivities in Figure 14.] As can be seen from Figure 14, the SSMF in full synthesis mode has a larger collecting area than any existing or planned millimeter-submillimeter instrument except the Nobeyama, Japan 45 m telescope (10) and has a much greater frequency capability than other instruments. Even the central 7-shooter of the SSMF will be one of the largest high frequency telescopes in the world and will have the advantages of being space based.

Some of the important areas of astronomical research to which a millimeter-submillimeter telescope can be applied are listed in Table 9. In general, the SSMF will provide a tremendous advance in our ability for millimeter-submillimeter wavelength observations of everything from our nearby Sun to the most distant quasars.

The Sun, our most important star, must be studied at millimeter wavelengths to probe the deepest part of its chromosphere and to investigate the magnetohydrodynamic processes of prominences, spicules, and flares. In the interplanetary medium, the sizes, shapes, compositions, and albedos of the asteroids can be determined and the complicated chemical reactions on comets can be observed. On the planets and their satellites

not only can their surface textures, temperatures, and albedos be determined, but the composition and dynamics of many atmospheric gasses can be investigated.

For example, the distribution and dynamics of carbon monoxide (CO) can be studied in the atmospheres of Mars and Venus (see, e.g., Figure 15; Schloerb, 1986); the atmospheres of the giant planets, Jupiter and Saturn, can be probed to greater depths than is possible at centimeter wavelengths; the composition of Saturn's rings, a continuing mystery, can be explored through thermal emission at mm wavelengths from the constituent particles; the vulcanism on Io can be monitored; and the massive atmosphere on Titan can be investigated. The heat flow in the planets and satellites can also be measured.

Galactic astronomy is one of the most active areas of millimeter-submillimeter wavelength research at the present time and will be greatly enhanced by the capability of the SSMF. The cores of the giant molecular clouds (GMCs) and the compact regions of star formation need detailed, high resolution studies of their composition, dynamics, temperature, and density to investigate this important birth phase of stars. For stars in intermediate stages of their life cycles, binary systems can become extremely active with large mass exchanges, accretion disks, and high velocity jets, while highly evolved stars lose mass at rapid rates by processes which are only poorly understood. The SSMF will be able to follow this evolution with its high resolution, high sensitivity, and spectral line capability.

The interstellar medium of gas and dust between the stars is known to be rich in atomic and molecular species and is in violent activity, contributing both to galactic dynamics and to stellar life cycles. All of these processes can be studied through the many transistions of molecules and neutral species known to be abundant throughout the Galaxy. For

example, over 50 molecules, including isotopic variations, are now known (see Table 10) with over 800 detected transitions -- even though the millimeter wavelength region is still poorly studied below 100 GHz and almost totally unexplored above that (see, e.g., Sutton et al., 1985; Blake et al., 1986). Many of the transitions increase in intensity as the square of the frequency, so that more and stronger emissions can be studied at shorter wavelengths. In the "mm-IR gap" between 300 GHz and 1 THz, essentially nothing has been explored but it will certainly be rich with molecular transitions from the unseen, "cold" component of the interstellar medium (see, e.g., Table 11).

Some of the more spectacular investigations which will become possible are the study of the molecular formation and disassociation regions in the interstellar shocks found in supernova remnants and in the high velocity winds of star formation regions. The most interesting examples of this last presently known are the so-called "bi-polar flows," where, by an unknown mechanism, some stars spew back into the interstellar medium high velocity molecular streams in two oppositely directed jets [see, e.g., Figure 16 (Goldsmith et al., 1984) and Figure 17 (Snell and Schloerb, 1985)].

Many of these interstellar processes, both thermal and non-thermal, are enhanced near the galactic center where the activity may involve accretion onto a massive core such as a black hole. The structure and dynamics of this vital region needs to be further investigated at millimeter wavelengths. The ultimate goal, of course, is the understanding of such complex processes as molecule formation and disruption, stellar wind and supernova injection, cloud formation and collapse, molecular species and isotopes, the large scale distribution of molecules and neutral atoms, and the formation, maintenance, and evolution of our Galaxy.

The SSMF with its high resolution and sensitivity will also provide a

major new observing capability for extragalactic studies. Past observations, in spite of their limitations, have shown that the distribution of molecular gas traced by the carbon monoxide (CO) distribution at 3 mm wavelength is drastically different from the neutral hydrogen (HI) distribution measured at 21 cm wavelength [see, e.g., Figure 18 (Young and Scoville, 1983)]. Because molecules are tracers of a much larger fraction of the mass in a galaxy than the neutral hydrogen, these results require modification of our understanding of the mass distributions and dynamics of galaxies. Also, there is a close correlation between the CC in a galaxy and its optical morphological type, implying a direct relation to the active regions of star formation. In order to investigate these tentative relations further, however, the much higher resolution and sensitivity of the SSMF is required for these distant objects.

Not only can the broad distributions of molecules like CO be investigated with this new observing capability, high resolution and sensitivity will give the possibility of studying individual giant molecular clouds (GMCs), the most massive entities in a galaxy, in other stellar systems. Much more information is needed on their structure, chemical composition, relation to galactic type, evolution, and dynamics.

Preliminary studies of the far-infrared emission surveyed by the Infrared Astronomy Satellite (IRAS) during its short operational lifetime show a strong correlation between IR emission and mm-wave emission [see, e.g., Figure 19 (Young et al., 1986)] so that low resolution IRAS maps can be used to pinpoint individual GMC complexes in other galaxies [see, e.g., Figure 20 (Habing et al., 1984)] for more detailed study at millimeter-submillimeter wavelengths. Thus, with a permanent observing facility such as the SSMF, many galaxies which are known to be strong infrared emitters can be mapped in detail to study their GMCs and star formation regions. Particularly, for a number of interacting galaxies which IRAS has shown to

be bright infrared sources, only the SSMF will have the resolution to be able to study the location and origin of the emission in detail. Additionally, material which is too cold to have been detected by IRAS can be mapped.

Outside of galaxies, the SSMF will allow investigation of a number of cosmological questions. Some Big Bang models predict fluctuations in the 3° K background (which peaks at about 1 mm) on the order of 10^{-4} which is related to the formation of galaxies in the initial expansion of the universe. Also, the Sunyaev-Zeldovich effect (scattering of 3° K photons by the hot gas in clusters of galaxies) needs to be measured far more accurately. Combining the millimeter information with x-ray observations of the same hot intra-cluster gas can be used to determine values for the distance scale (Hubble Constant) and the expansion parameter (q_o) of the universe.

In the very distant and powerful extragalactic, non-thermal radio emitting objects such as active galactic nuclei (AGNs), quasars (QSOs), and low frequency variables (LFVs), the SSMF can carry out high frequency intensity monitoring and spectrum determination up to and through the mm - IR gap. A number of spectral variations related to the energy generation mechanism in these enigmatic objects are thought to occur in this wavelength range. For example, 99% of all quasars are not strong radio emitters but have (presumably) non-thermal optical and x-ray emission similar to the "radio loud" quasars. This deviation must be explained.

Finally, to probe deeply into the optically thick cores of the very compact AGNs, QSOs, and LFVs for investigation of the energy generation mechanisms and the origin of the apparently faster than light "superluminal" motions, millimeter Very Long Baseline Interferometry (VLBI) can be carried out between the SSMF and ground-based millimeter telescopes to obtain extremely high resolution and rapid mapping capability.

CONTROL AND CORRELATION

Since weight, space, and power limitations on the Space Station will be severe, only the minimum amount of data processing capability can be placed in orbit. This will need to satisfy two basic requirements: 1) a general purpose computer to monitor, point, and control the physical operations of the array antennas and their related subsystems (a control computer), and 2) a special purpose computer to steer, collect, correlate, and compress the data streams arriving from each of the array antennas (a correlator). Input to the control computer will be loaded periodically either by the Space Station personnel or by an uplink from the ground and output from the correlator will be returned to the ground either by down-loading through a radio data channel or by physical return of a high density recording medium (tapes?; laser disks?) on a resupply vehicle such as the Space Shuttle.

All data analysis facilities will be located on the ground and, because of the similarity of the output data to that from existing or planned radio arrays (e.g., the VLA and the VLBA), these already exist to a certain extent in the form of VAX computers running AIPS software packages at many locations throughout the world. Since the data analysis facilities are not likely to be incorporated into the Space Station, they will not be discussed further in this consideration of the space based components.

Control Computer. The constraints on a central control computer are not severe. Its main functions involve: 1) coordinate conversions from Earth or celestial coordinate frames to that of the Space Station and then to the altitude-azimuth coordinates of the individual antennas, 2) fringe rotation and delay calculations, and 3) system monitoring. Also, since most tasks will be interpolated between central control computer updates by locally (at each dish) placed microprocessors, the average communication rates will

be quite low, on the order of only a few hundred bits per second. Even the more complicated coordinate conversions and fringe and delay calculations should involve no more than a few tens of kilo-flops, implying that a high quality microcomputer will be able to adequately perform the control computer function.

Correlator. The requirements for the special purpose computer which correlates the outputs from a large array of antennas, especially when including spectral line capability, can exceed all reasonable bounds if all desirable observing programs are to be satisfied. Therefore, to provide a basis for design and cost development, we will specify an operationally useful maximum data capability to be attained.

Specified quantities:

1) Number of antenna elements = 37;
2) Maximum continuum bandwidth (10 channels of 100 MHz bandwidth each) = 1 GHz;
3) Maximum sampling rate (one bit sampling) = 200 MHz;
4) Full polarization = R,L or X,Y;
5) Maximum number of spectral line channels = 512.

Derived quantities:

1) Number of bit streams/antenna/polarization at 200 MHz rate = 10;
2) Number of baselines (37x36/2) = 666;
3) Number of complex correlations/baseline/bit stream for full continuum polarization = 4;
4) Number of complex correlations/baseline for line observations with no polarization and 100 MHz maximum bandwidth = 512.

Yield:

1) Number of complex correlators for full polarization, full 1 GHz bandwidth continuum observations = 26,640 (x2 sine and cosine correlators);
2) Number of complex correlators for no polarization, 100 MHz maximum bandwidth, 512 channel line observations = 340,992. (x2 sine and cosine correlators).

As is obvious from the above numbers and as is also the experience in existing arrays, the requirements for spectral line observations dictate the size of the needed correlator (as well as the size of the post-correlation data reduction load) and useful astronomical line observations are known to exist which would require an arbitarily large correlator. However, with the specifications discussed above, most types of desirable line and continuum observations can be performed well with ∿700,000 simple (∿350,000 complex) correlators. This is a reasonable size, being approximately twice as large as the existing VLA correlator which contains 373,242 simple correlators and is based on late 1970's and early 1980's technology.

The master computer for the correlator need not be a large or sophisticated machine since it will mainly be used to calculate to high precision (rather than at very high speed) and to load control information to more locally based microprocessors in the correlator. An existing minicomputer of the VAX 750 class could provide the needed performance, perhaps with an associated array processor (AP) for performing Fourier transformations.

COST ESTIMATES

Since the design for the Space Station is still in its very initial stages and since not even its basic structure and form are well defined (let alone its exact cost or the cost of adding facilities to it once it is completed), it is difficult to estimate the cost of the SSMF. However, we will attempt to obtain a crude value by estimating the cost of constructing such a facility on the ground and then adopting an arbitrary multiplying factor to obtain a rough estimate of the cost in space. This "space factor" we will define to be 10x and its magnitude (as well as the magnitude of the estimates for the various components of the SSMF) will need to be refined as more information becomes available. It must further be emphasized that even the estimates for a ground based cost do not represent a proper engineering study and cannot be regarded as accurate to better than a factor of $\sim$2.

The technology already exists for construction (on the ground) of essentially all components of the SSMF (with the possible exception of receivers where, for the highest frequencies of $\sim$1 THz, development of low noise heterodyne systems to replace presently available bolometers is desirable). Therefore, the greatest uncertainties and cost driving factors are those related to constructing and operating systems in space.

The construction of a 10.4 m dish with a surface accuracy of $\sim$10 μm has been demonstrated in the laboratory by Leighton (see, e.g., Leighton, 1978). Such accuracy is sufficient for 1 THz operation, even with some degradation in an operational environment, and is certainly achievable for the smaller 5 m dishes of the SSMF. A conservative cost estimate, considering the large number to be produced, is $\sim$\$100K per dish.

Since the individual array elements are relatively small and have a half power beam width of $\sim$15" even at 1 THz ($\sim$5" for the 7-shooter), the

pointing requirements are not extremely severe and ∿1" pointing accuracy will be sufficient. On the other hand, for Earth sensing the ability to rapidly raster scan large areas of the Earth's surface will require relatively robust antenna mounts. Thus, as an initial estimate, it is assumed that a dish mount will cost as much as the dish itself, with a cost factor of ∿3x greater for the larger mount of the 7-shooter.

Because development is taking place rapidly in very high frequency receivers, cost estimates are extremely uncertain. Also, many individual receivers will be needed to provide the 5 beam and dual polarization capability of each dish at each frequency so that small errors in the cost estimate for each receiver will be important and possible savings due to the mass production of receivers are unknown. With these caveats in mind, it is estimated that receivers will cost on the average ∿$10K each and will be needed for ∿10 frequency bands. The cost of cryogenics to cool each receiver package to ∿4° K must also be added (estimated at ∿$50K each).

Each antenna will need both digital and analogue electronics systems which are estimated to cost ∿$150K each. The individual antenna feeds, because they will have to be built very precisely and in arrays of 5 horns per feed, are estimated to cost ∿$50K each.

Because the SSMF will be a connected array, only one hydrogen maser clock will be needed. It will then allow the combined array to be used for VLBI observations together with ground-based stations. The clock is estimated to cost ∿$200K.

The control computer can be quite small and is estimated to cost no more than ∿$100K. The correlator, on the other hand, is a very significant article of hardware and software development and construction and cannot be constructed for less than ∿$3M.

Communications, IF, and data transmission lines throughout the array, with its maximum extent of only ∿100 m from the center, are relatively

inexpensive and estimated to cost ∿$100K.

Engineering and design costs should not be strongly dependent on where the equipment is to be placed and are estimated to be ∿$2M without the "space cost factor" of 10. Software development while extensive, can partially be drawn from that available for existing ground-based systems and also should not have a space cost factor. It is estimated that ∿20 manyears of effort will be needed at ∿$50K per manyear or ∿$1M total.

These rough initial estimates are listed in Table 12 and yield a total cost of $\sim\$0.6 \times 10^9$. We feel that these are conservative estimates and that a more exact study may yield lower values.

SUMMARY

It is clear that a high frequency array telescope such as the SSMF constructed on the planned Space Station will equal or exceed in capability any existing or planned ground based instrument. Also, because of its placement outside of the Earth's atmosphere, it will be able to extend research into previously unexplored frequency ranges. The SSMF will serve as a test bed for developing and proving new techniques for constructing and operating large structures and large instruments in space and it will provide new capability for surveillance of ground and space based targets. The SSMF will open vast new possibilities for scientific and engineering research in a number of areas such as Earth sensing, atmospheric studies, deep space communications, and astronomy.

For surveillance, the ability to operate at numerous frequencies with high sensitivity and high resolution means that the SSMF can search for, detect, identify, and track targets over tens of thousands of square kilometers against an Earth or sea background with better than 100m resolution under all weather conditions. Space based targets, depending on

their surface properties, can also be detected and tracked against the celestial background. This being accomplished entirely with passive radiometry or bistatic radar using space based or airborne transmitters, avoids the telltale radiation and possibility for jamming inherent to radar.

For Earth sensing, the SSMF is sensitive to the different emissive properties of crops, forest, land, sea, and man made structures and to their differing effects on polarization. Sea and land temperature differences, soil and crop moisture variations, types of ground cover, and the presence and age of surface snow and ice will all stand out clearly.

For atmospheric studies, detailed investigation of the middle atmosphere will be greatly enhanced by the SSMF. The distribution, dynamics, and density of many important atmospheric constituents such as water and ozone can be mapped in detail and numerous trace elements can be studied both for their own properties and for their diagnostic capabilities as tracers of other elements. This information will shed light on such important questions as the destruction of the Earth's ozone shield, the operation of gravity waves for mixing in the middle atmosphere, and the long term accumulation of carbon dioxide associated with such possibly serious climate modifiers as the greenhouse effect. All of this new information will enhance atmospheric modeling for possible improvement in long range weather and climate forcasting.

For studies of the ionosphere, analysis of the D-region chemistry and dynamics with the SSMF can lead to a strategically important predictive capability for long range radio communications; and for determining the infrared target background, the SSMF can provide global, long term measurement of the major atmospheric infrared active molecular species and aid the development of a background predictive capability.

For deep space communications beyond the orbits of Jupiter and Saturn,

existing radio telescopes provide insufficient gain for reliable data transmission at high bit and low error rates. Only the SSMF, with its large collecting area, low noise receivers, and high directivity will be able to provide the performance necessary for rapid image transmission from probes of the outer Solar System.

Last, but certainly not least, the SSMF will represent an advance for millimeter-submillimeter radio astronomy as great or even greater than that represented by the Hubble Space Telescope (HST) for optical astronomy. It will place in Earth orbit an array of telescopes which has greater sensitivity and resolution at high radio frequencies than any existing instrument. With the advantage of being above the disturbance of the Earth's atmosphere, it will exceed in capability even the largest millimeter-submillimeter telescopes being planned and will be able to extend observations into frequency ranges unavailable to ground-based instruments. The SSMF will attack myriad problems in astronomy ranging from the properties of the Sun's surface, to the atmospheres of the planets and their satellites, to the structure and composition of the interstellar medium and the origin of the enigmatic processes of star formation and birth, to the structure of the center of our own Galaxy the Milky Way, to the properties of the numerous nearby galactic systems and the distant quasars. Spectral line observations will allow investigation of the chemistry and physics of all of these regions, opening up the first new possibility for high quality imaging with high sensitivity and high spectral and spatial resolution in an unexplored wavelength range since those provided by the Einstein x-ray satellite and the IRAS infrared satellite.

All of these aspects, as well as a discussion of some of the data handling and processing techniques and a very preliminary cost estimate have been presented. However, with a facility so unique and so powerful,

it is obvious that not all parts of it or all uses of it can possibly be covered or even conceived of in a short report. More detailed discussion and development is obviously called for on all aspects of the design, construction, and use of the SSMF.

REFERENCES

Barrett, A. H., Lada, C. J., Palmer, P., Synder, L. E., and Welch, W. J. 1983, in Report of the Subcommittee on Millimeter- and Submillimeter-Wavelength Astronomy, submitted to the National Science Foundation Astronomy Advisory Committee in April 1983.

Blake, G. A., Sutton, E. C., Masson, C. R., and Phillips, T. G. 1986, Astrophys. J. Suppl., Vol. 60, p. 357.

Brasseur, G. and Solomon, S. 1984, in Aeronomy of the Middle Atmosphere: Chemistry and Physics of the Stratosphere and Mesosphere, (Reidel: Dordrecht).

Brejcha, A. G. 1980, Microwave J. 23, No. 1, 25.

Crane, R. K. 1976, in Methods of Experimental Physics 12, Part B, 177.

Edelson, R. E., Madsen, B. D., Davis, E. K., and Garrison, G. W. 1979, Science 204, 913.

Goldsmith, P. F., Snell, R. L., Hemeon-Heyer, M., and Langer, W. D. 1984, Astrophys. J. 286, 599.

Habing, H. J., Miley, G., Young, E., Baud, B., Bogges, N., Clegg, P. E., deJong, T., Harris, S., Raimond, E., Rowan-Robinsion, M., and Soifer, B. T. 1984, Astrophys. J. (Letters) 278, L59.

Hollinger, J. P. 1985, NRL Millimeter Imaging Program, private communication.

Hollinger, J. P. and Lo, R. C. 1984, Determination of Sea Surface Temperature with N-Ross, NRL Memorandum Report 5375.

JPL 1985, Jet Propulsion Laboratory Atmospheric Transmission Program, communicated by T. G. Phillips.

Leighton, R. B. 1978, California Institute of Technology Technical Report.

Lintz, J. and Simonett, D. S. 1976, Remote Sensing of Environment, (Addison-Wesley: London).

Moore, J. 1984, in Janes' Fighting Ships, (Janes: London).

Pampaloni, P. and Paloscia, S. 1985, in Remote Sensing Instrumentation Technology for Science and Applications - IGARSS '85, (IEEE: New York), p. 619.

Rogstad, D. H. and Shostak, G. S. 1972, Astrophys. J. 176, 315.

Schloerb, F. P. 1986, in ESO-IRAM-Onsala Workshop on (Sub) millimeter Astronomy, in press.

Snell, R. L. and Schloerb, F. P. 1985, Astrophys. J. 295, 490.

Sutton, E. C., Blake, G. A., Masson, C. R., and Phillips, T. G. 1985, Astrophys. J. Suppl. 58, 341.

Taylor, J. W. R. 1984, in Janes': All the World's Aircraft, (Janes: London).

Ulaby, F. T., Moore, R. K., and Fung, A. K. 1981, Microwave Remote Sensing - Active and Passive: Volume I, (Addison-Wesley: London).

Ulaby, F. T., Moore, R. K., and Fung, A. K. 1982, Microwave Remote Sensing - Active and Passive: Volume II, (Addison-Wesley: London).

Young, J. S., Schloerb, F. P., Kenney, J., and Lord, S. 1986, Astrophys. J., in press.

Young, J. S. and Scoville, N. Z. 1983, in Kinematics, Dynamics, and Structure of the Milky Way, W. Shuter, ed. (Reidel: Dordrecht), p. 367.

Waters, J. W., 1976 in Methods of Experimental Physics 12, Part B, 142.

Table 1 — Assumed System Parameters

Number of single antennas			30		
Single antenna size			5 m		
Antenna efficiency			0.5		
Number of multiple dish antennas (7-shooter)			1		
Number of sub-elements			7		
Sub-element size			5 m		
Antenna efficiency			0.5		
Frequency (ν) coverage			10 GHz to 1 THz		
Wavelength (λ) coverage			3 cm to 300 microns		
Polarization			Full - R,L or X,Y		
Bandwidth			1 GHz		
System temperature	10 GHz 20 K	30 GHz 50 K	100 GHz 100 K	300 GHz 200 K	1 THz 500 K
Maximum baseline			200 m		
Individual arm lengths			100 m		
Array form			"T"		
Number of single antennas per arm			10		
Altitude			500 km		
Number of feeds per antenna, staggered array			5		

Table 2 — Capability

Collecting area (7-shooter)	137 m^2
Collecting area (Full array of 37 dishes)	726 m^2
Equivalent single dish diameter (7-shooter)	13.2 m
Equivalent single dish diameter (Full array of 37 dishes)	30.4 m
Sensitivity (1σ) on sky at 300 GHz with 30^m integration (7-shooter)	3.8 mJy; 0.43 mK
Sensitivity (1σ) on sky at 300 GHz with 30^m integration (Full array of 37 dishes)	0.7 mJy; 13.6 mK
Resolution on sky at 300 GHz (7-shooter)	∿15"
Resolution on sky at 300 GHz (Full array)	∿1"
Sensitivity (1σ) on Earth at 10 GHz with 0.5^s integration (Full array of 37 dishes in pushbroom mode)	0.6 K
Sensitivity (1σ) on Earth at 10 GHz with 60^s integration (Full array of 37 dishes in tracking mode)	0.06 K
Resolution on Earth at 10 GHz at 50° viewing angle (7-shooter)	1.4 x 2.2 km
Resolution on Earth at 10 GHz at 50° viewing angle (Full array)	110 x 340 m
Single horn field of view on sky at 300 GHz	40"
Single horn field of view on Earth at 10 GHz at 50° viewing angle	4.4 x 6.9 km
Field of view with staggered array of 5 feeds	5x

Table 3 — Ratio R of Target to Sea Brightness Temperature Contrast (ΔT_b) and SSMF System Noise Temperature (T_{sys}) ($R \equiv \Delta T_b/T_{sys}$)

Surface Conditions		Atmosphere†	Cloud/rain thickness	Ratio R at		
Temperature	Relative Humidity			10 GHz	35 GHz	90 GHz
10°C	30%	Clear	-----	-0.8	-0.5	-0.4
20°C	50%	Clear	-----	-0.7	-0.4	-0.2
20°C	50%	Cumulus clouds	1 km	-0.7	-0.3	-0.1
30°C	100%	Clear	-----	-0.7	-0.3	0.0
30°C	100%	Cumulus conjestus	3 km	-0.2	+0.03	0.0
20°C	100%	Light rain, 2.5 mm hr^{-1}	1 km	-0.7	-0.2	0.0
30°C	100%	Heavy rain, 25 mm hr^{-1}	2 km	-0.3	0.0	0.0

†Atmospheric absorption and scattering data are from Waters, 1976 and Crane, 1976.

Table 4 — SSMF Downlooking Parameters at 50° Incidence Angle

Frequency (GHz)	Single beam half-power width (km)	Maximum half-power width of 5-beam pattern (km)	Interferometric resolution (m)	Survey rate at orbital speed [pushbroom] ($km^2\ s^{-1}$)	Integration per point for push-broom mode (sec)	Contrast sensitivity ΔT_b for pushbroom mode[1] (3σ) (K)	Contrast sensitivity ΔT_b for pushbroom mode[2] (3σ) (K)
10	4.4 x 6.9	22	110 x 480	165	0.46	0.6	0.6
35	1.3 x 2.0	6.3	30 x 140	47	0.13	1.7	2.6
90	0.5 x 0.8	2.5	12 x 50	18	0.05	5.0	15.0

Frequency (GHz)	Single beam half-power width (km)	Maximum half-power width of 5-beam pattern (km)	Interferometric resolution (m)	Survey area in tracking mode (km^2)	Integration per point in tracking mode (sec)	Contrast sensitivity ΔT_b for tracking mode[1] (3σ) (K)	Contrast sensitivity ΔT_b for tracking mode[2] (3σ) (K)
10	4.4 x 6.9	22	110 x 480	120	60	0.06	0.06
35	1.3 x 2.0	6.3	30 x 140	10	60	0.08	0.12
90	0.5 x 0.8	2.5	12 x 50	1.6	60	0.14	0.43

[1]Under good weather with surface conditions of 20°C, 50% relative humidity, and clear skies.
[2]Under poor weather with surface conditions of 20°C, 100% relative humidity, and light rain.

Table 5 — Earth Sensing Applications

	Typical ΔT_b at 10 GHz (K)	Possible requirements	
		Moderate resolution	High resolution
Oceanography			
Sea surface roughness	5	X	
Sea surface temperature	1	X	
Pollution mapping	20	X	X
Hydrology			
Soil Moisture	50	X	
Soil roughness	30	X	
Snowcover mapping	50	X	X
Flood mapping	150		X
Agriculture			
Vegetation cover	30	X	X
Crop growth	30	X	
Economic Surveying			
Man-made structures	10-150		X

Table 6 — SSMF Earth Sensing Parameters

Frequency (GHz)	Mode	Resolution	Total swath width (km)	3σ Brightness sensitivity ΔT_b (K)
10	Full interferometric, high resolution (CM3)	110 x 340 m	22	2
	Single dish total power, moderate resolution (CM1)	4.4 x 6.9 km	617	0.1
35	Full interferometric, high resolution (CM3)	20 x 100 m	6.3	5
	Single dish total power, moderate resolution (CM1)	1.3 x 2.0 km	188	0.2
90	Full interferometric, high resolution (CM3)	12 x 40 m	2.5	11
	Single dish total power, moderate resolution (CM1)	0.5 x 0.8 km	75	0.3

Table 7 — Molecular Constituents of the Middle Atmosphere Measurable with the SSMF

Species	Measurement Range
H_2O	20 - 90 km
HO_2	30 - 50 km
H_2O_2	30 - 45 km
OH	30 - 50 km
O_3	20 - 90 km
ClO	30 - 45 km
CO	30 - 100 km
NO	30 - 80 km
NO_2	30 - 45 km
N_2O	10 - 35 km
Kinetic temperature	20 - 100 km
Atmospheric pressure	35 - 70 km

Table 8 — Voyager X-Band Telecommunications Parameters

Transmitting Element	
Carrier frequency	8.4 GHz
Maximum power	21 Watts
Antenna diameter	3.7 m
Aperture efficiency	38%
Bit rate (high)	115 kb s^{-1}
Bit rate (low)	44.8 kb s^{-1}
Receiving Elements	
Goldstone (DSN-14)	
Antenna diameter	64 m
Aperture efficiency	34%
System temperature	28.5 K
System losses	16%
Very Large Array (VLA)	
Effective antenna diameter	130 m
Approximate aperture efficiency	50%
System temperature	50 K
Approximate system losses	16%

Table 9 — Objects Potentially Visible with an Aperture Synthesis Array of 1" Resolution, 1 MHz Bandwidth, and 10^3 m^2 Collecting Area†

Type of Source	Physical size	Maximum distance at which detectable	Detectable at the distance of
Small proto-planetary disc	20 AU	20 pc	Nearby stars
Large proto-planetary disc	100 AU	100 pc	Taurus and ρ-Oph clouds
Maser emitting clumps	200 AU	200 pc	Nearest clouds
Post-shock cooling layer	1000 AU	1 kpc	Gould's Belt clouds
Interstellar disc	0.1 pc	20 kpc	Entire Galaxy
Bipolar flow (molecular jet)	1 pc	200 kpc	Entire Galaxy
Massive molecular cloud core	10 pc	2 Mpc	Local group of galaxies
Forming cluster or association	10 pc	2 Mpc	Local group of galaxies
Giant molecular cloud	100 pc	20 Mpc	Virgo cluster of galaxies
Nuclear disc	400 pc	80 Mpc	Virgo super-cluster
Galactic spiral arm	1 kpc	200 Mpc	Nearby galaxy clusters
Molecule rich galaxy (M82)	10 kpc	2000 Mpc	z = 0.2 quasars

†From Barrett et al., 1983.

Table 10 — Detected Species and Line Survey Parameters†

CO	HCN	H_2S	HC_3N
CN	HNC	HNCO	CH_3CN
NO	HCO^+	H_2CO	CH_3CCH
CS	HCS^+	H_2CS	C_2H_3CN
SiO	OCS	H_2CCO	C_2H_5CN
SO	SO_2	HCOOH	$HCOOCH_3$
C_2H	HDO	CH_3OH	CH_3OCH_3

Source: OMC-1	Coverage: 208 - 263 GHz
Sensitivity: $\lesssim$0.2-0.3 K	Resolution: 1 MHz
Lines Identified: $\gtrsim$825	Unidentified Lines: 32
Isotopes Detected:	H,D, ^{12}C, ^{13}C, ^{14}N, ^{15}N, ^{16}O, ^{17}O, ^{18}O, ^{28}Si, ^{29}Si, ^{30}Si, ^{32}S, ^{33}S, ^{34}S, ^{35}Cl

†From Sutton et al., 1985 and Blake et al., 1986.

Table 11 — Rotational Envelope Maxima and Fundamental Transition Frequencies of Some Interstellar Molecules†

Molecule, envelope maximum	ν (GHz)	Hydride, lowest transition	ν (GHz)
CO J=5→4	576.3	NaH J=1→0	289.9
HCO^+ J=6→5	535.1	H_3O^+ $J_K=2_1\rightarrow1_1$	307.2
HCN J=6→5	531.7	MgH $^2\Sigma^+$ J=1/2,N=1→0	343.0
H_2CO $J(K_pK_0)=6_{05}\rightarrow5_{05}$	434.5	H_2D^+ $J(K_pK_0)=1_{10}\rightarrow1_{11}$	372.4
CS J=8→7	391.8	MgH^+ J=1→0	377.5
CH_3OH $J_K=8_0\rightarrow7_0A$	386.7	AlH J=1→0	377.6
SiO J=8→7	347.3	LiH J=1→0	444.0
HCS^+ J=8→7	341.3	CH_2 $J(K_pK_0)=3_{03}\rightarrow2_{12}$	444.9
SO $N_J=8_8\rightarrow7_7$	337.6	H_2S $J(K_pK_0)=1_{11}\rightarrow0_{00}$	452.4
H_2CS $J(K_pK_0)=9_{09}\rightarrow8_{08}$	308.7	SiH^+ J=1→0	453.0
H_2CCO $J(K_pK_0)=11_{0,11}\rightarrow10_{0,10}$	222.2	NH_2 $J(K_pK_0)=1_{10}\rightarrow1_{01}$	461.5
SO_2 $J(K_pK_0)=11_{1,11}\rightarrow10_{0,10}$	222.0	PH $^3\Sigma^-$N=1→0	498.0
CH_3CN $J_K=12_0\rightarrow1_{10}$	220.7	HBr J=1→0	500.6
SiS J=12→11	217.8	CH $^2\pi_{3/2}$,J=3/2$^2\rightarrow\pi_{1/2}$,J=1/2	532.7
CH_3O $CH_3J(K_pK_0)=11_{1,11}\rightarrow10_{0,10}$	209.5	NH_3 $J_K=1_0\rightarrow0_0$	572.5
OCS J=14→13	170.3	HCl J=1→0	625.9
HC_3N J=16→15	145.6	SiH $^2\pi_{1/2}$,J=3/2→1/2	660.0
$HCOOCH_3$ $J(K_pK_0)=13_{0,13}\rightarrow12_{0,12}$	142.8	CH^+ J=1→0	835.1
C_2H_5CH $J(K_pK_0)=16_{0,16}\rightarrow15_{0,15}$	139.3	NH $^3\Sigma^-$N=1→0	974.5
HC_5N J=29→28	77.2	H_3O^+ $J_K=1_0\rightarrow0_0$	984.6

†From Sutton et al., 1985 and Blake et al., 1986.

Table 12 — Cost Estimates (K$)

Per interferometer element		
5 m dish	$ 100	
Mount & guidance equipment	$ 100	
Feeds	$ 50	
Cooled receivers (10 bands x 5 receivers x 2 polarizations x $10K each)	$1,000	
Cryogenic refrigerator (4° K)	$ 50	
Electronics (digital & analogue)	$ 150	
Total per antenna	$1,450	
Subtotal for 30 antennas		$43,500
Seven-shooter		
7 x 5 m dishes @ $100K each	$ 700	
Mount & guidance equipment	$ 300	
7 x feeds @ $50K each	$ 350	
Cooled receivers (10 bands x 5 receivers per dish x 2 polarizations x 7 dishes x $10K each)	$7,000	
7 x cryogenic refrigerators (4° K) @ $50K each	$ 350	
7 x electronics (digital & analogue) @ $150K each	$1,050	
Subtotal for 7-shooter	$ 9,750	$ 9,750
Hydrogen maser observatory clock		$ 200
Control computer including peripherals		$ 100
Correlator		$ 3,000
Communications lines, IF transmission lines		$ 100
Subtotal		$56,650
x 10 for space application		$566,500
Engineering and design		$ 2,000
Software development		$ 1,000
Total		$569,500

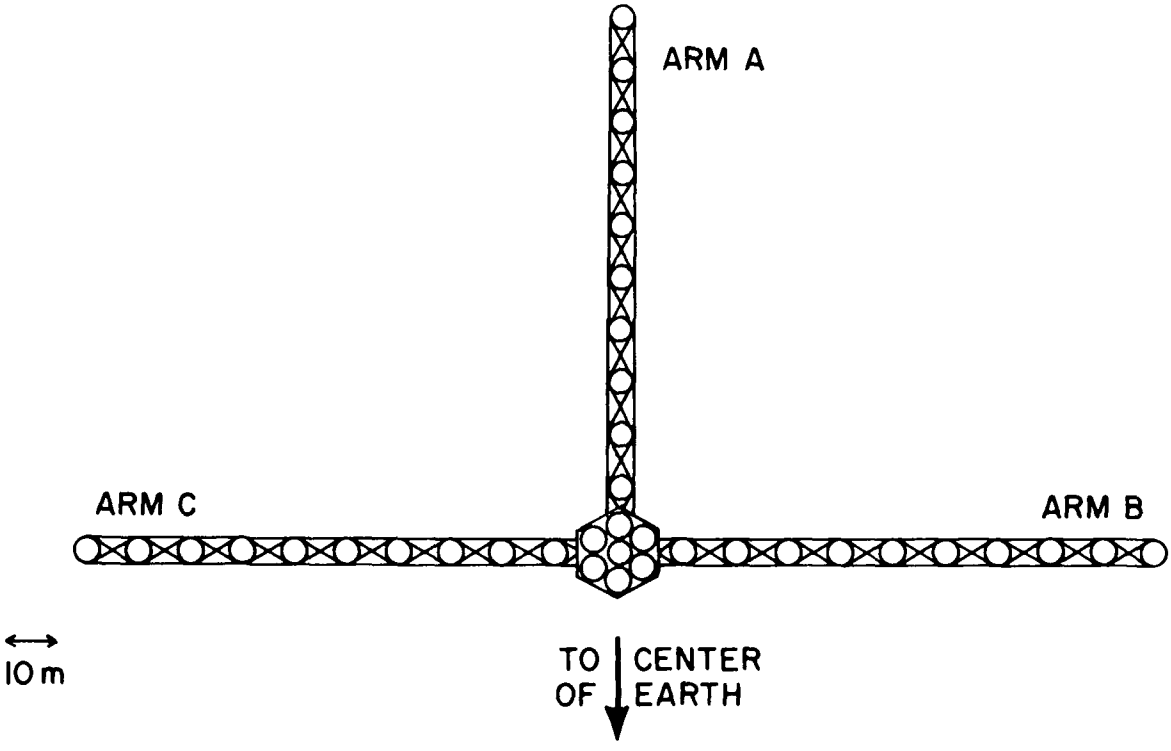

Fig. 1 — Schematic diagram of the SSMF viewed anti-parallel to its instantaneous velocity vector assuming gravity gradient stabilization along its vertical arm (Arm A). All three arms (Arms A, B, & C) are perpendicular to the instantaneous velocity vector which is tangential to the orbital path. 30 dishes, each 5 m in diameter are spaced at 10 m intervals in a "T" configuration with each arm supporting 10 dishes and being ~100 m long. A central large survey antenna (7-shooter) contains 7 dish elements, each 5 m in diameter. All individual dishes and the 7-shooter are fully and independently steerable.

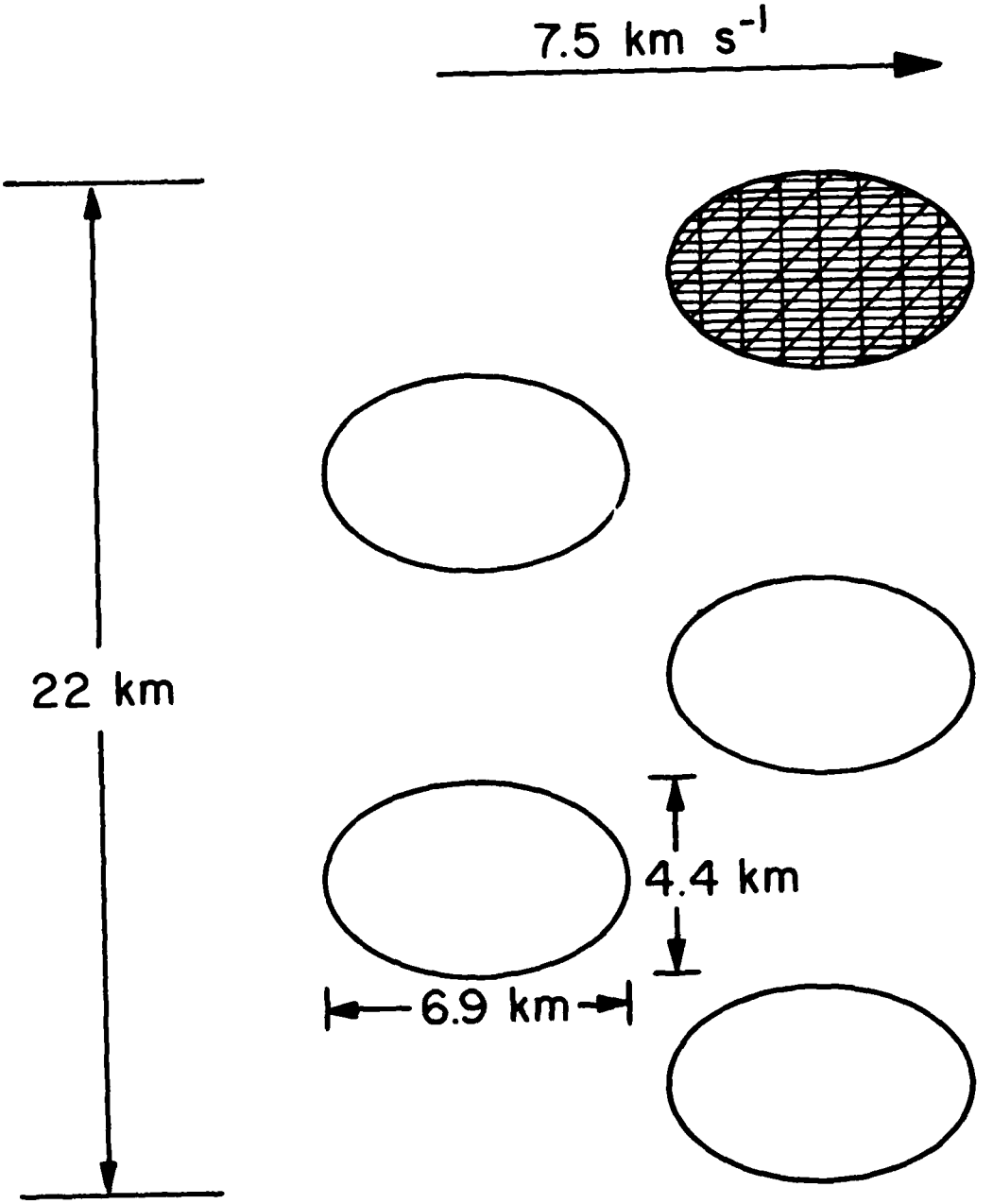

Fig. 2 — Primary beam pattern of the SSMF with 5 feeds per antenna at 10 GHz projected on to the Earth's surface at an incidence angle of 50°. Diameters of the ellipses correspond to the half-power beam width. The interference pattern which results from correlating the full array permits high resolution mapping within each beam area and is illustrated schematically in the top beam.

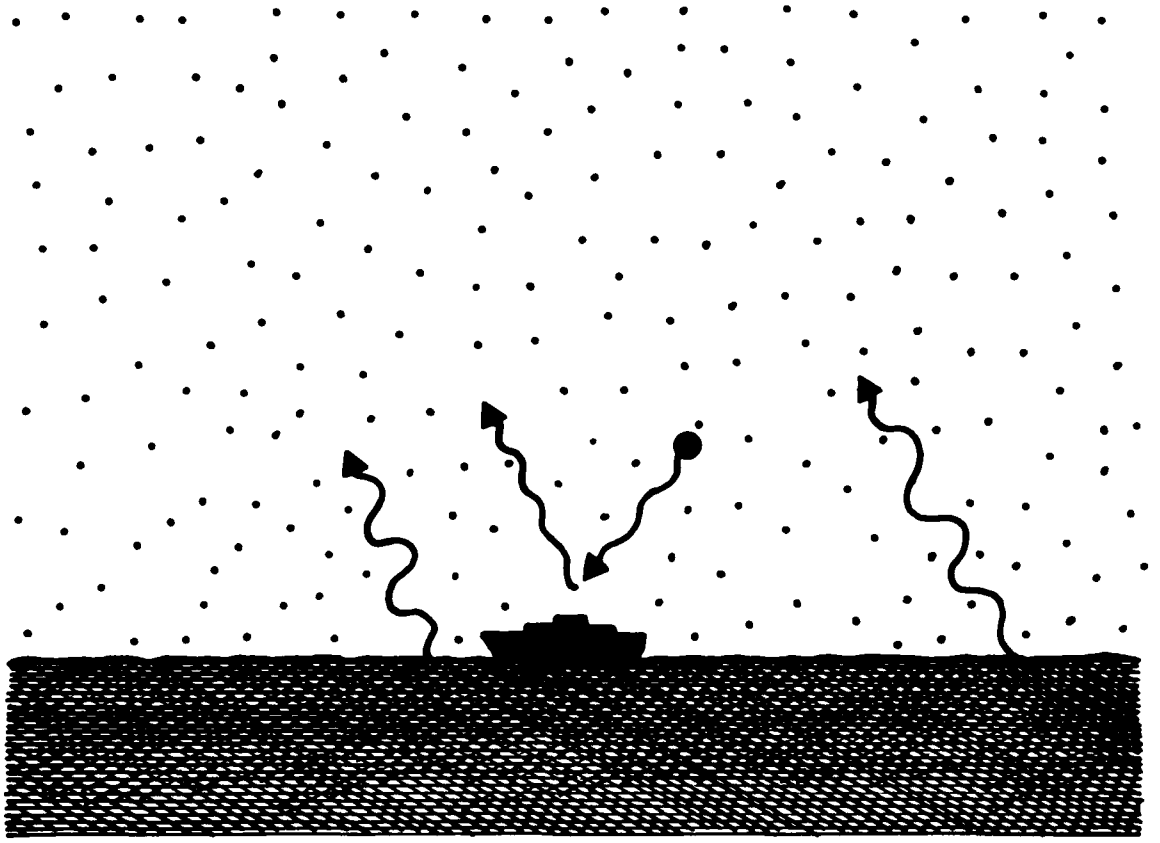

Fig. 3 — Schematic diagram of target detection. The SSMF detects the contrast between a metallic ship reflecting "cold" atmospheric emission upward and the surrounding "warm" sea emission.

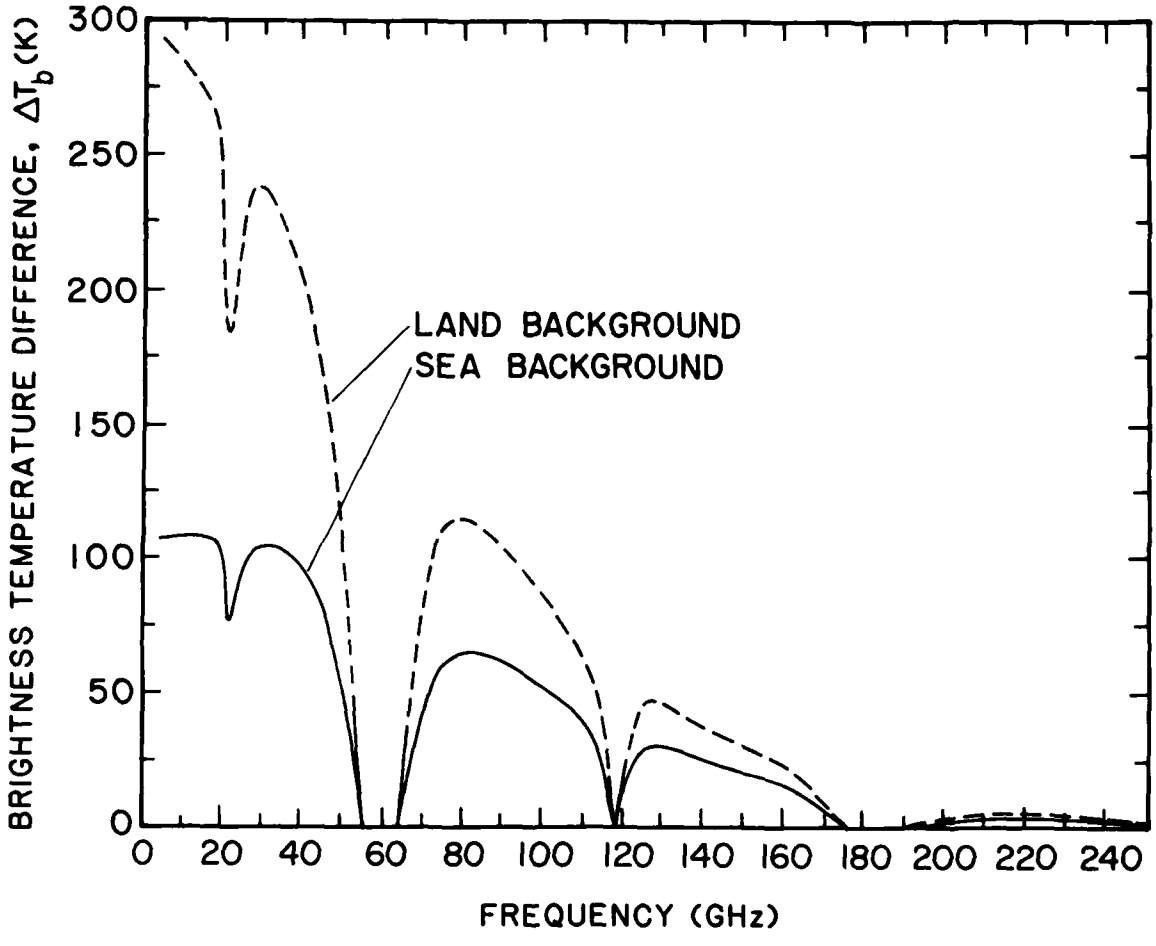

Fig. 4 — Apparent brightness temperature difference (ΔT_b) under good weather conditions between a reflecting target and a land (dashed curve) or sea (solid curve) background at normal incidence as a function of observing frequency (Hollinger, 1985).

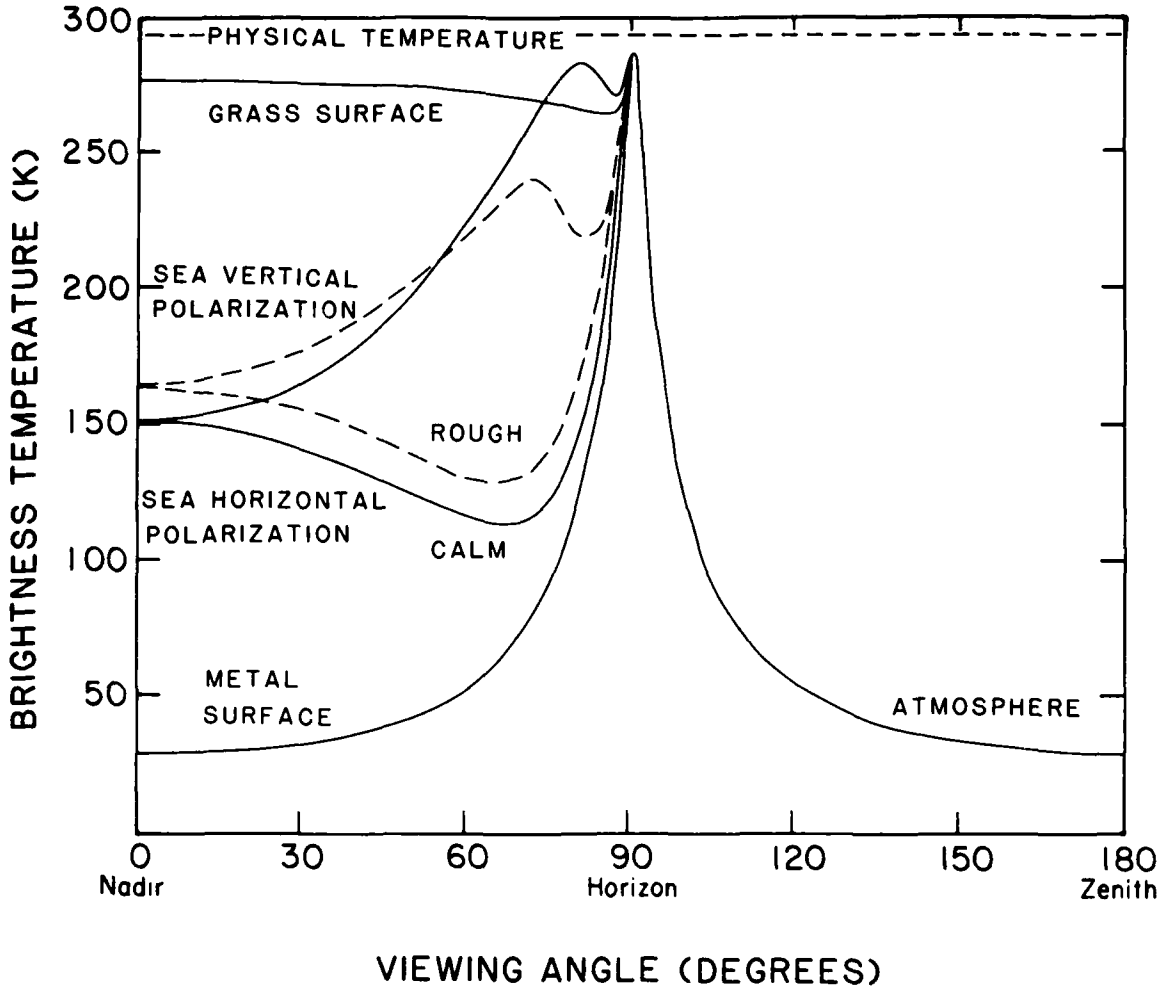

Fig. 5 — Brightness temperature (T_b) of the sea, grass covered land, and a standard atmosphere with light clouds near 35 GHz. The effects of sea roughness on the vertical and horizontal components of the linear polarization are also shown (Hollinger, 1985).

WAKES

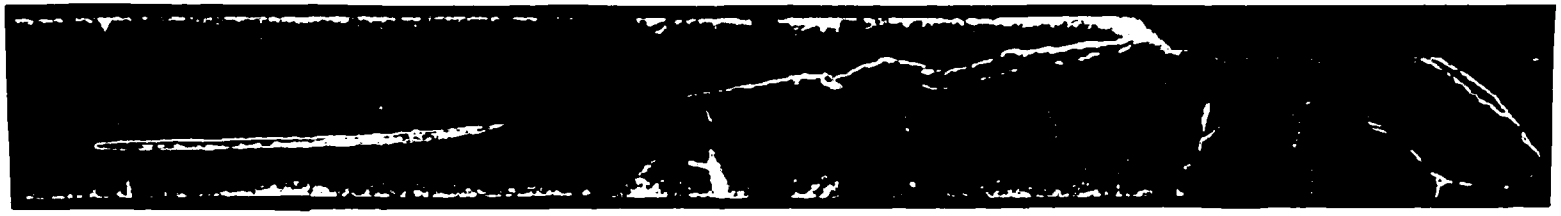

90 GHz

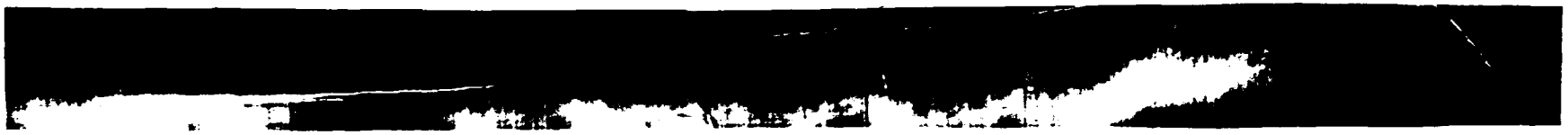

Visual

15 km

Altitude = 940 meters

Surface Resolution = 16 meters

NRL

Fig. 6 — False color photograph of a harbor mapped at 90 GHz from a test plane flying at 940 m. The resolution is 16 m and the color scale is relative, with warmer temperatures shown in red and cooler temperatures shown in blue. A visual photograph of the same area is also shown for comparison purposes (Hollinger, 1985).

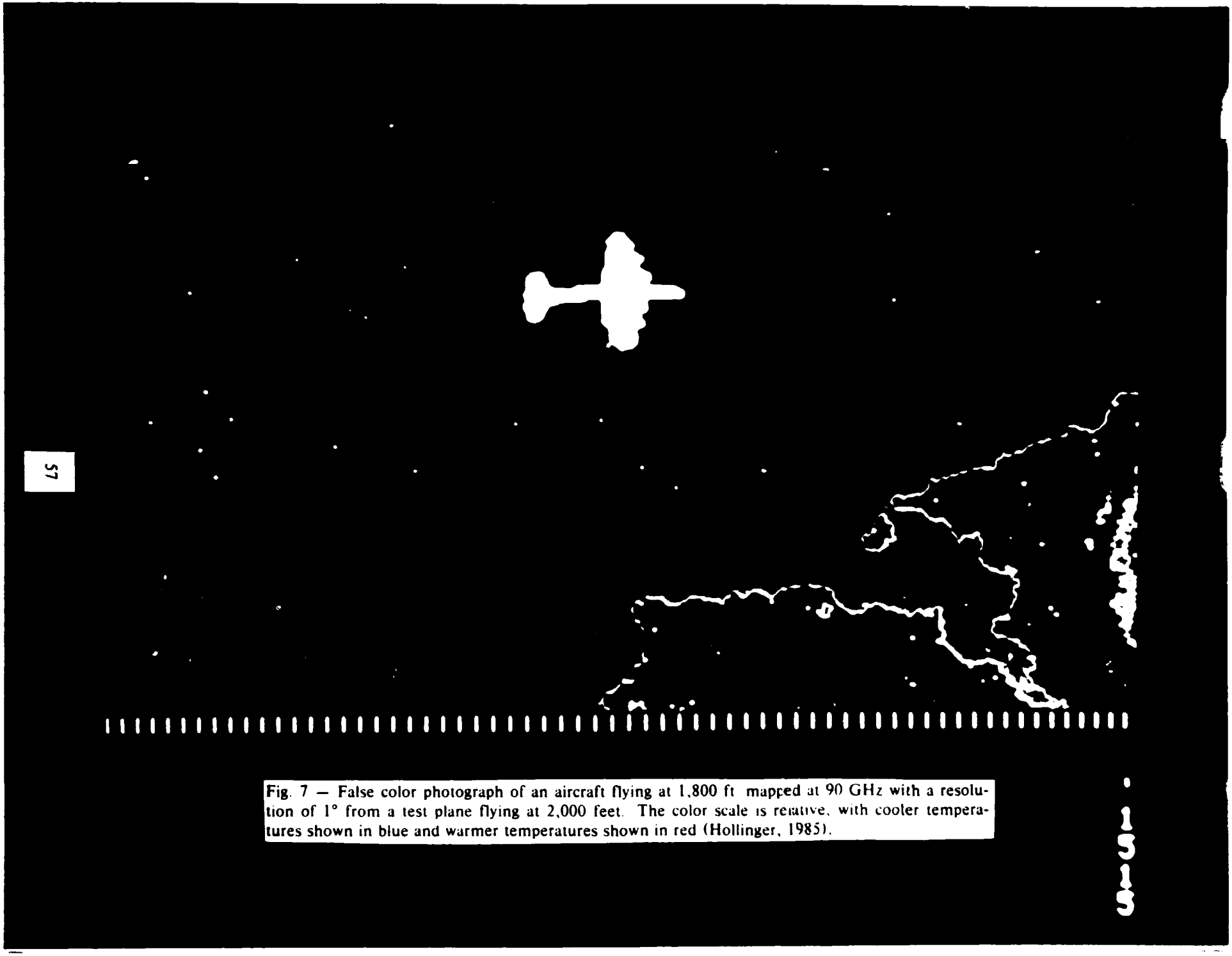

Fig. 7 — False color photograph of an aircraft flying at 1,800 ft mapped at 90 GHz with a resolution of 1° from a test plane flying at 2,000 feet. The color scale is relative, with cooler temperatures shown in blue and warmer temperatures shown in red (Hollinger, 1985).

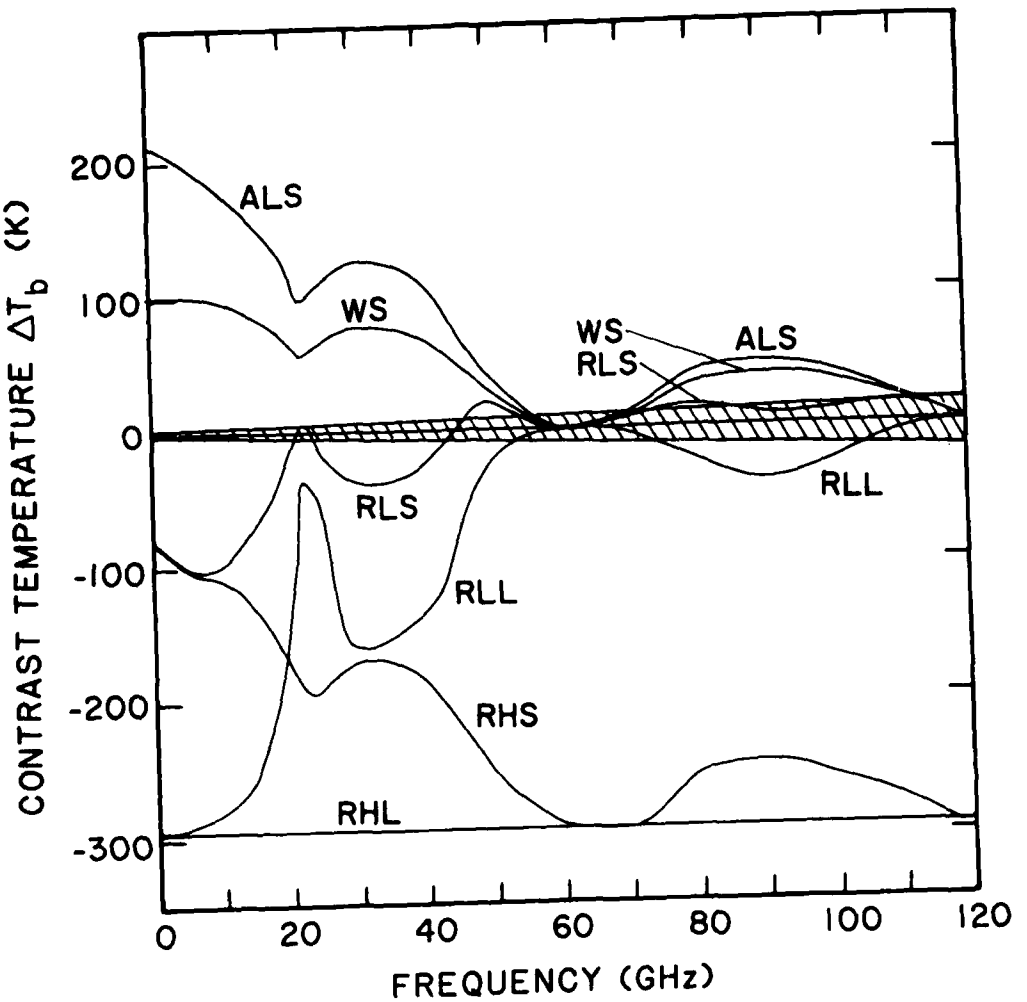

Fig. 8 — Contrast brightness temperature (ΔT_b) in degrees Kelvin (no beam dilution) for a number of target situations as a function of frequency for the relatively poor surface conditions of 20° C, 100% relative humidity, and light rain. [RLS = reflecting target at low altitude (or on the sea) against a sea background; RHS = reflecting target at high altitude against a sea background; RLL = reflecting target at low altitude (or on the land) against a land background; RHL = reflecting target at high altitude against a land background; ALS = absorbing target at low altitude (or on the sea) against a sea background; WS = wake on the sea's surface.] The 3σ sensitivity limit of the SSMF in pushroom mode (OM1) is shown as the crosshatched area.

58 - Blank

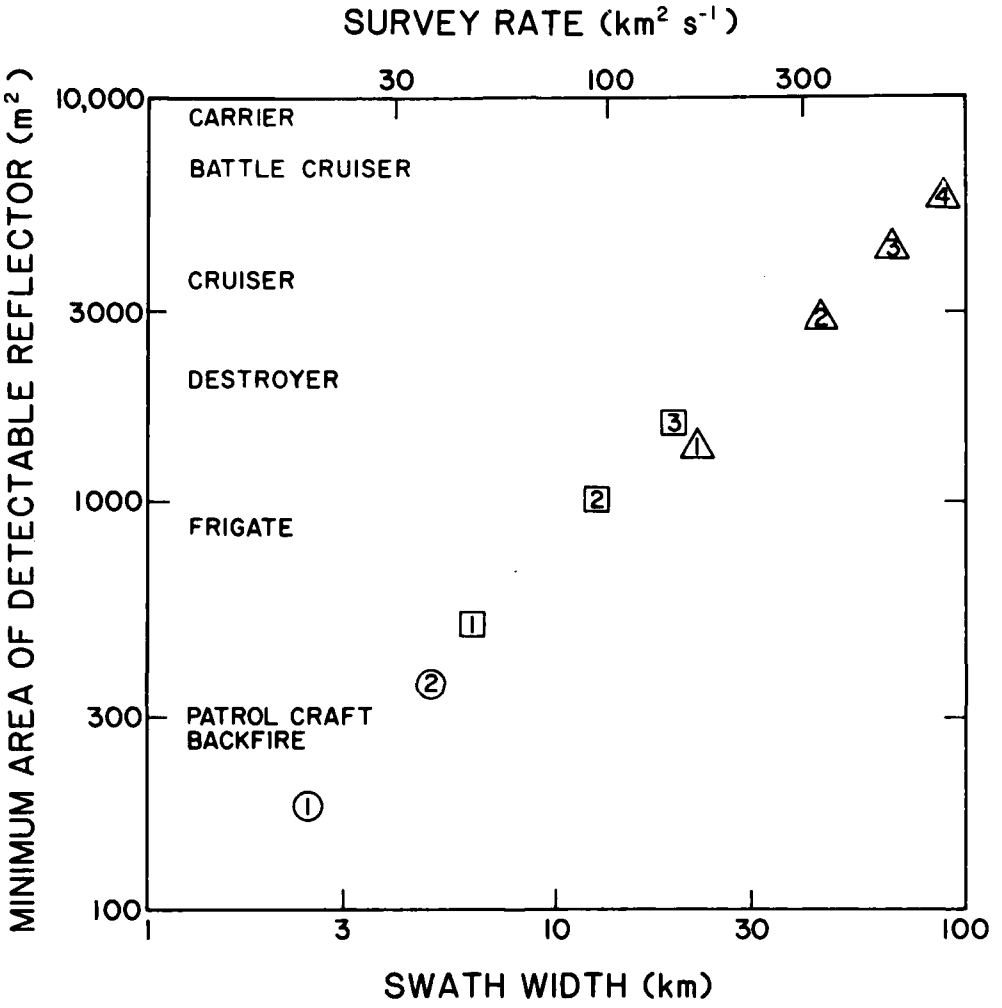

Fig. 9 — Sensitivity limits (5σ) in pushroom mode (OM1) for various array and sub-array (CM2) configurations at several frequencies under good weather conditions. Triangles denote 10 GHz observations, squares 35 GHz, and circles 90 GHz. Numerals indicate the number of independent subarrays used. 1 implies the use of all 37 antennas in a full synthesis mode (CM3) while 2, 3, and 4 indicate the splitting of the SSMF into two, three, or four independent sub-arrays (CM2), respectively. The areas of various metallic, reflecting targets (Moore, 1984; Taylor, 1984) are indicated along the vertical axis.

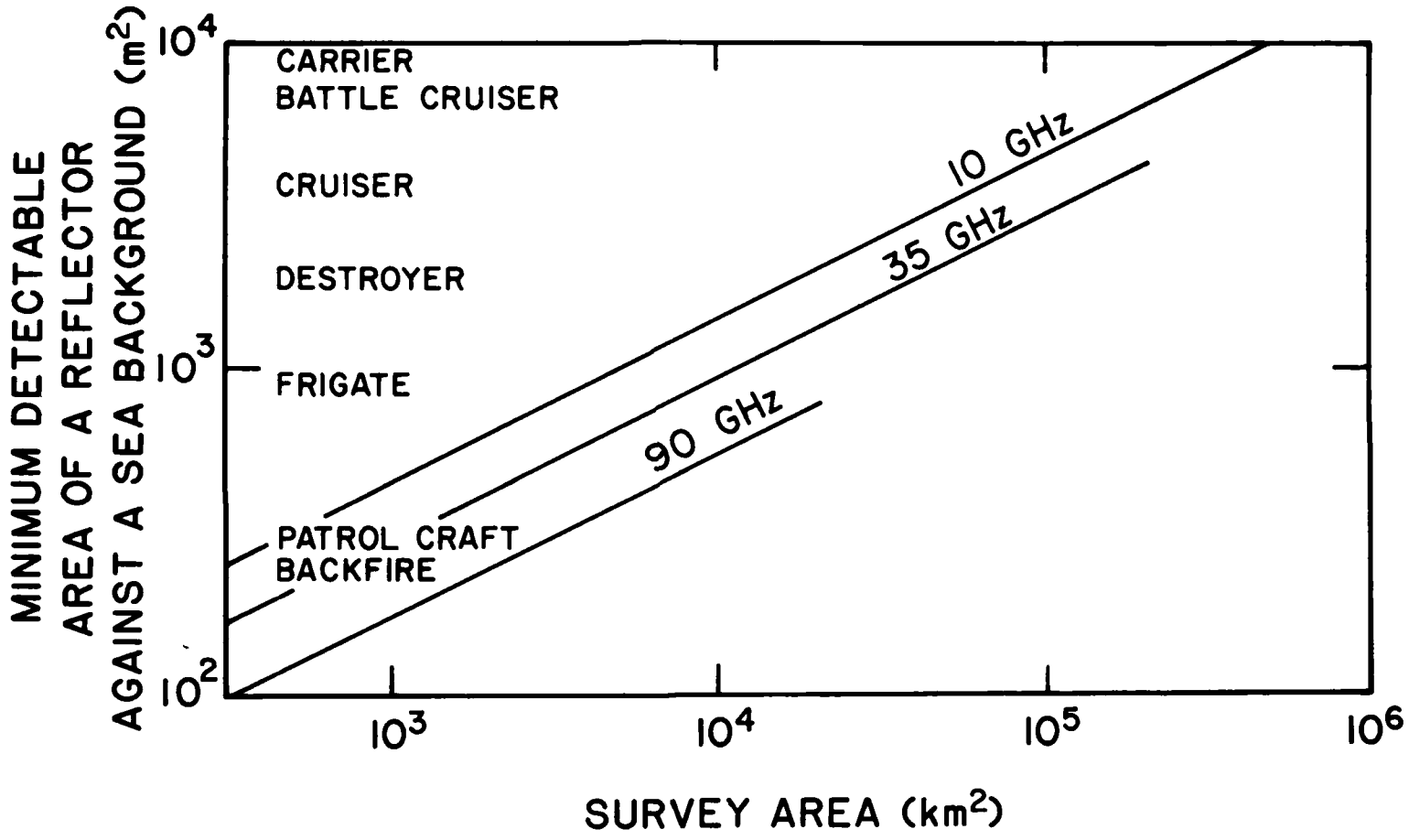

Fig. 10 — Sensitivity limits (5σ) for detecting metallic, reflecting targets against a sea background when rastering (OM3) large areas with the SSMF under good weather conditions. Various possible targets (Moore, 1984; Taylor, 1984) are shown. Upper limits to the 35 and 90 GHz survey areas correspond to the maximum areas which can be surveyed during one orbital pass with a maximum antenna nodding rate of 1 Hz.

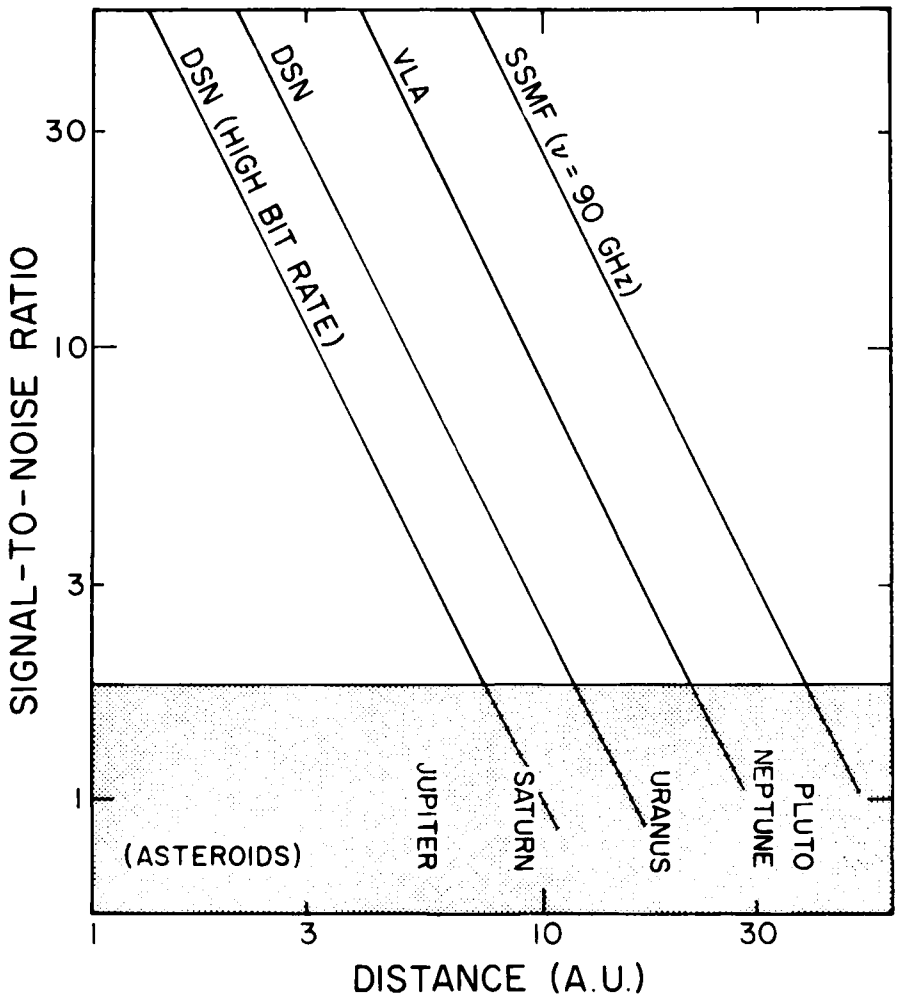

Fig. 11 — Signal-to-noise ratio (dimensionless) vs distance in Astronomical Units (A.U.) (1 A.U. = 1.5×10^8 km), for various deep space communications systems. [DSN = Deep Space Network 64 m antenna (Goldstone); VLA = Very Large Array; SSMF = Space Station Microwave Facility.] The transmitter characteristics are those of the Voyager spacecraft, although for the far right curve a frequency of 90 GHz is assumed. For the curves labelled Goldstone and VLA the frequency is 8.4 GHz (Voyager X-band telecommunications channel). The bit rate is 44.8 kb s^{-1}, except where noted as high bit rate, which is 115 kb s^{-1}. The shaded region corresponds to a bit error rate in excess of 0.5%, the tolerance for Voyager imaging data.

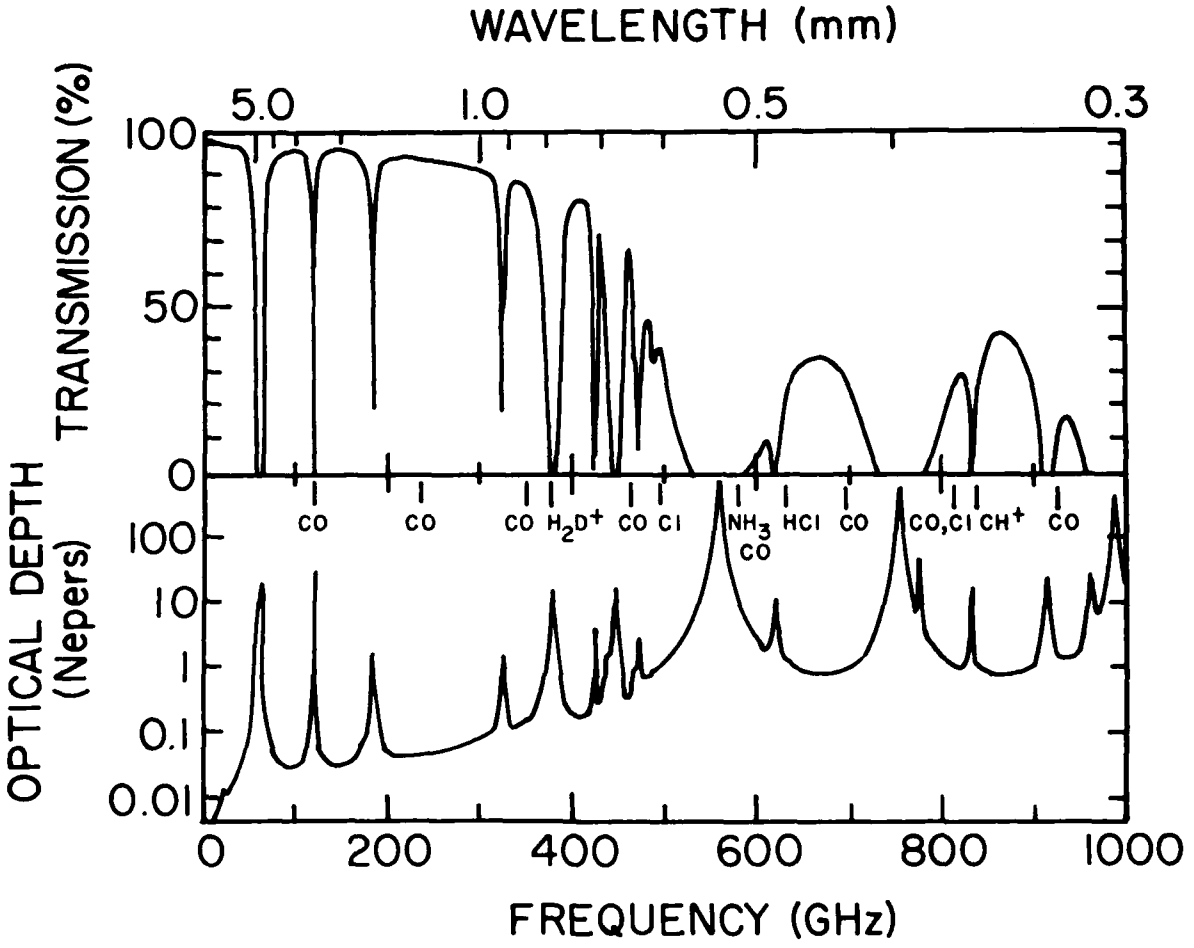

Fig. 12 — Transmission and optical depth of the atmosphere for 1.5 mm of precipitable water vapor from probably the best ground-based observing site, the top of Mauna Kea, Hawaii at a height of 4,200 m. As is evident from the figure, observations up to 300 GHz (1 mm wavelength) experience some degradation, from 300 GHz to 500 GHz only a few relatively poor observing "windows" are available, and for frequencies > 500 GHz observations are essentially impossible (JPL, 1985).

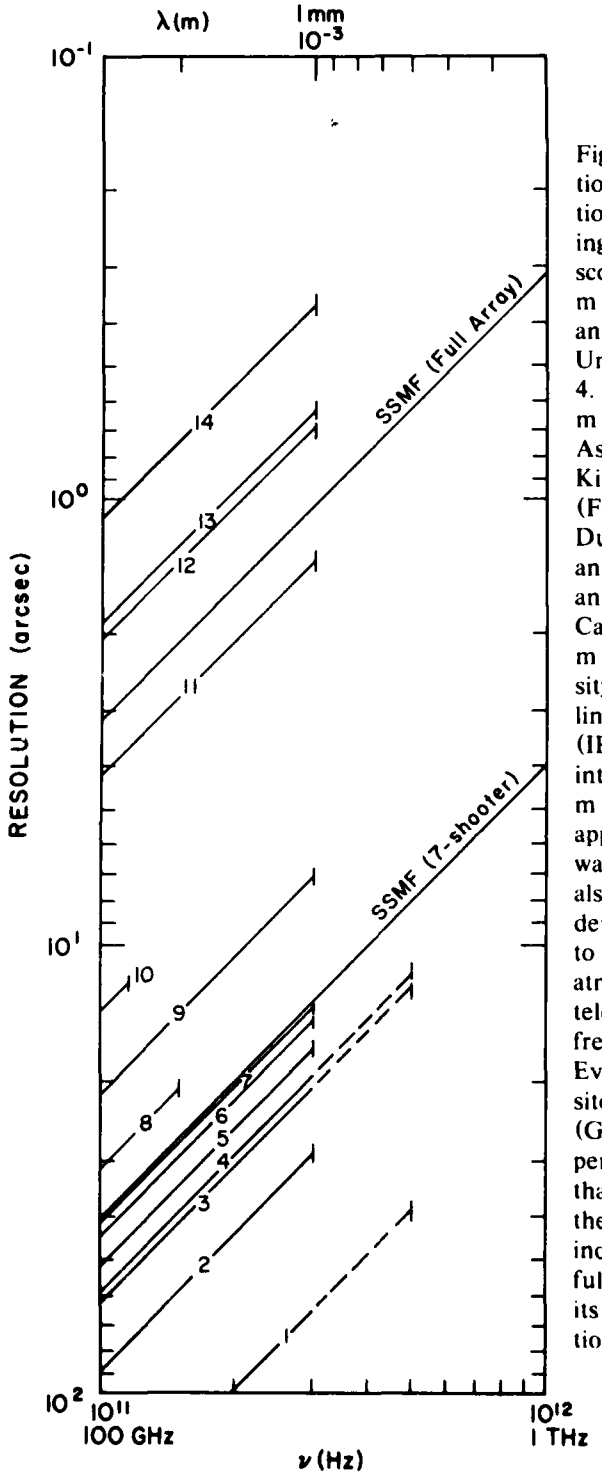

Fig. 13 — The maximum resolution (best resolution at top, poorest resolution at bottom) as a function of frequency (wavelength) possible with existing or planned millimeter-submillimeter radio telescopes. [1. Infrared Telescope Facility (IRTF) 3.2 m telescope; 2. Bell Telephone Laboratory 7 m antenna; 3. planned Max Planck Institut — University of Arizona 10 m submillimeter antenna; 4. planned California Institute of Technology 10.4 m submillimeter antenna; 5. National Radio Astronomy Observatory (NRAO) 12 m antenna on Kitt Peak; 6. Five College Radio Observatory (FCRAO) 13.7 m antenna; 7. planned British-Dutch 15 m antenna; 8. Onsala, Sweden 20 m antenna; 9. German-French (IRAM) 30 m antenna; 10. Nobeyama, Japan 45 m antenna; 11. California Institute of Technology 3 element (10.4 m each) 150 m baseline interferometer; 12. University of California 3 element (6 m each) 300 m baseline interferometer; 13. planned German-French (IRAM) 3 element (15 m each) 320 m baseline interferometer; 14. Nobeyama, Japan 5 element (10 m each) 560 m baseline interferometer.] The approximate highest frequency (shortest wavelength) to which each telescope is useful is also shown. All ground based telescopes, independent of their location and surface quality are limited to frequencies <500 GHz (0.6 mm wavelength) by atmospheric absorption (see Figure 12) and most telescopes are limited by their surface accuracy to frequencies <300 GHz (>1 mm wavelength). Even for the highest quality antennas and observing sites, observations in the frequency range $300 < \nu$ (GHz) < 500 will only be possible on a few days per year under optimum observing conditions so that this frequency interval, even when within the theoretical capability of the instrument, has been indicated by a dashed line. The SSMF, both for full resolution observations and for surveying with its central 7-shooter, is unhindered by these limitations. (Data from Barrett *et al.*, 1983).

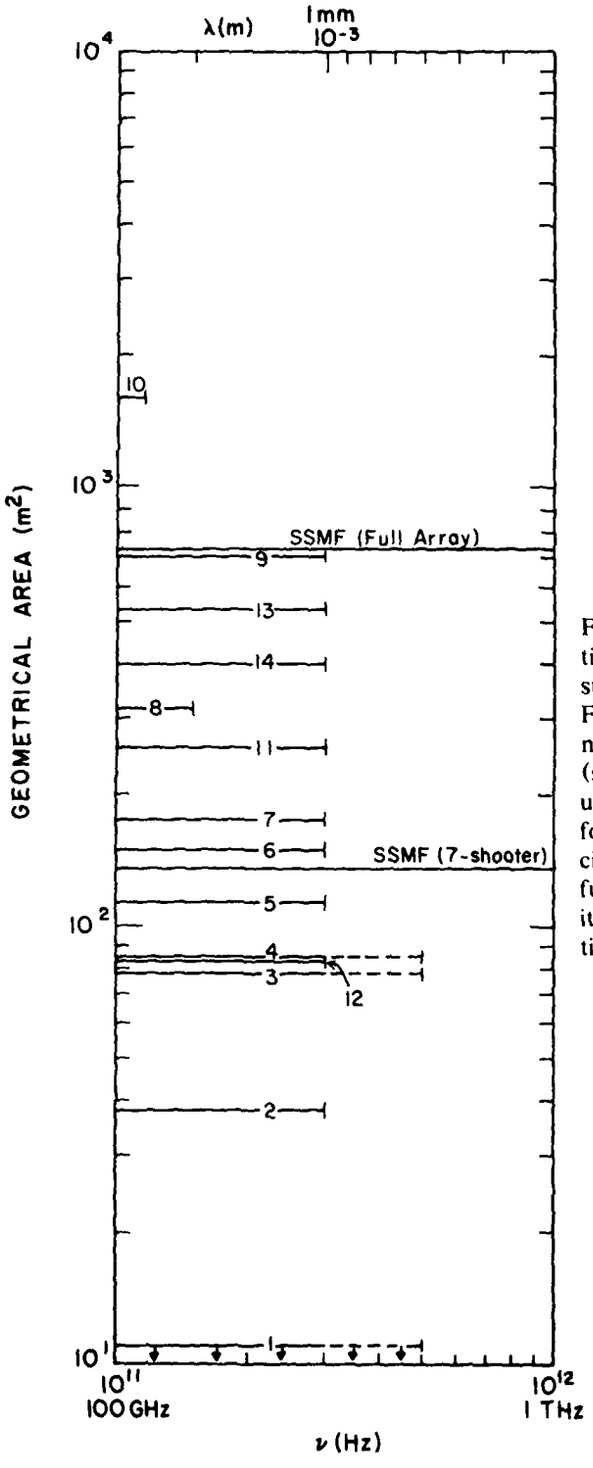

Fig. 14 — The geometrical areas (related to sensitivities) of existing or planned millimeter-submillimeter radio telescopes. [See the caption to Figure 13 for the key to the telescope identifying numbers.] The approximate highest frequency (shortest wavelength) to which each telescope is useful is also shown. [See the caption to Figure 13 for further discussion of the upper cutoff frequencies and atmospheric effects.] The SSMF, both for full sensitivity observations and for surveying with its central 7-shooter, is unhindered by these limitations. (Data from Barrett *et al.*, (1983).

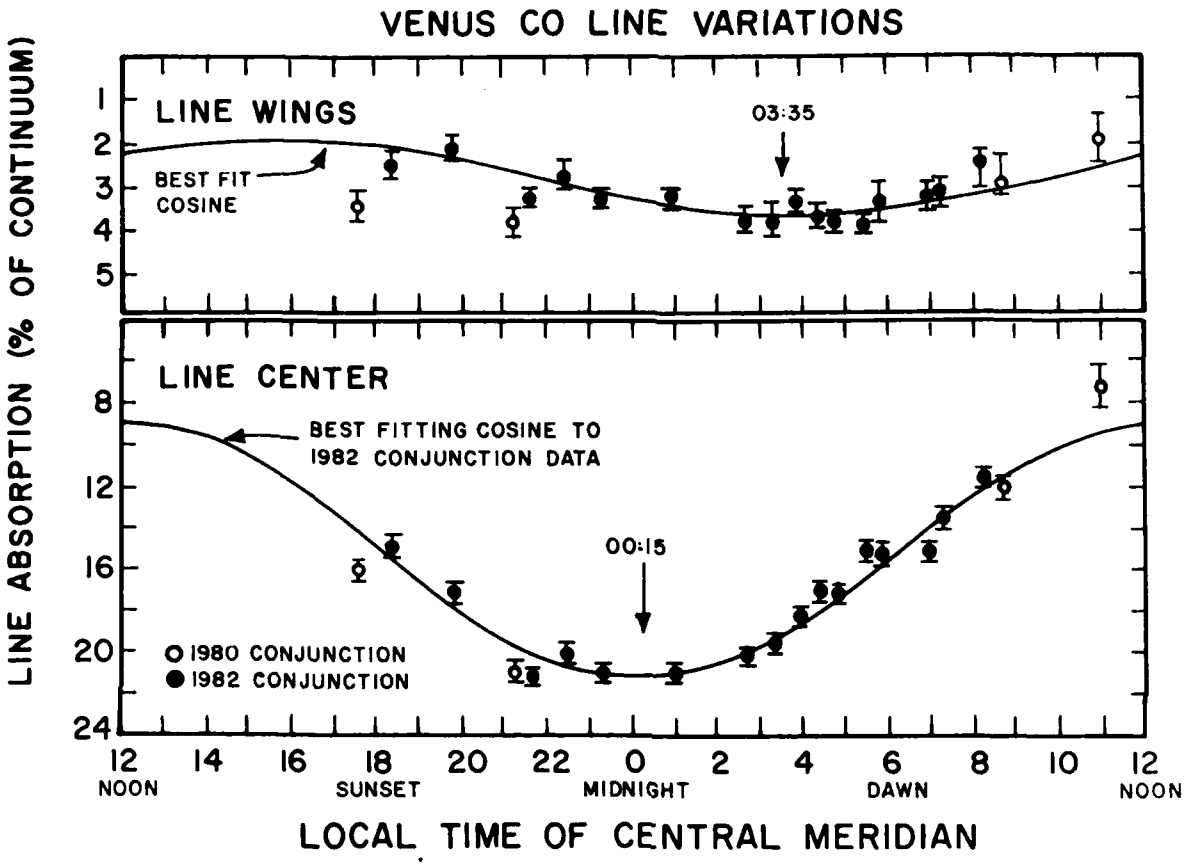

Fig. 15 — Results of monitoring the J=1-0 CO line in the Venusian atmosphere with the FCRAO telescope. The depth of the absorption line versus Venusian local time for the central median of the planet is plotted. The lower plot is for the line center, which traces variations of the CO abundance in the mesosphere (>90 km) and the upper plot is for the wings of the CO line which trace the CO abundance at altitudes between 80 and 90 km. (From Schloerb, 1986.)

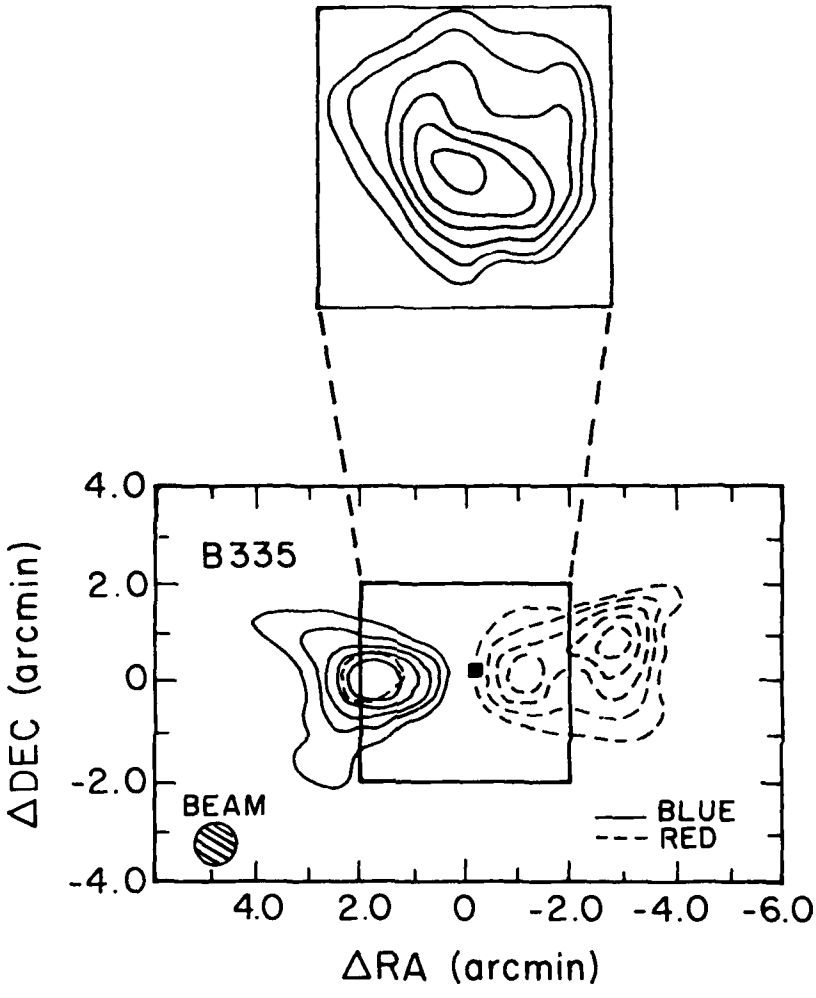

Fig. 16 — The lower contour map shows the integrated CO intensity measured with the FCRAO telescope in the redshifted (dashed line) and blueshifted (solid line) high-velocity wings, revealing a well-collimated bipolar outflow in B335. The filled square indicates the location of the far-infrared source powering the outflow. The inset shows a map of the CS J=2→1 emission around the far-infrared source. Clearly, the far-infrared source is at the center of the dense cloud core but no significant elongation is seen in the CS emission that might suggest the presence of a disk that collimates the outflow. (From Goldsmith *et al.*, 1984)

68 - Blank

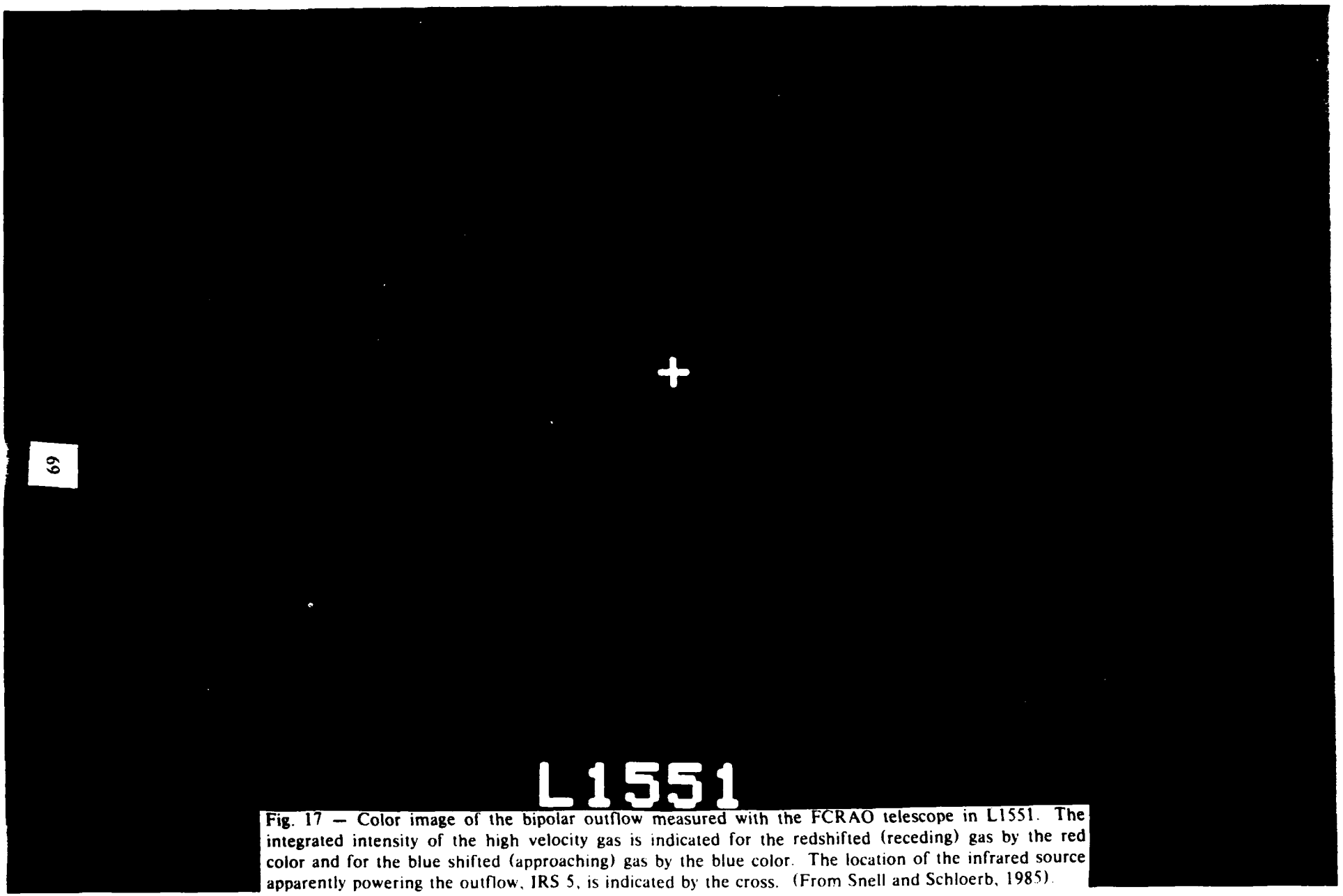

Fig. 17 — Color image of the bipolar outflow measured with the FCRAO telescope in L1551. The integrated intensity of the high velocity gas is indicated for the redshifted (receding) gas by the red color and for the blue shifted (approaching) gas by the blue color. The location of the infrared source apparently powering the outflow, IRS 5, is indicated by the cross. (From Snell and Schloerb, 1985).

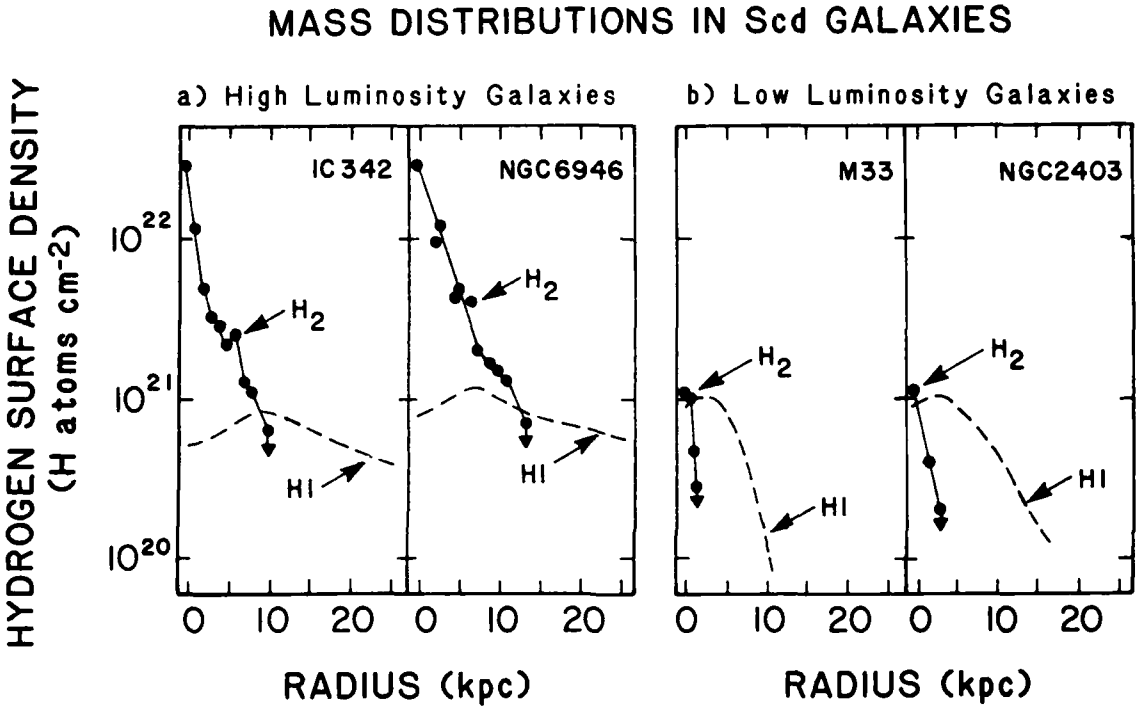

Fig. 18 — Radial distributions of molecular hydrogen (H_2) determined from carbon monoxide (CO) observations with the FCRAO telescope at 3 mm wavelength compared with the radial distributions of atomic hydrogen (HI) (Rogstad and Shostak, 1972) in 4 Scd galaxies of high and low optical luminosity. The high luminosity galaxies show more CO in their centers than the low luminosity galaxies, even though all 4 galaxies have similar central and maximum HI surface densities. (From Young and Scoville, 1983.)

70 - Blank

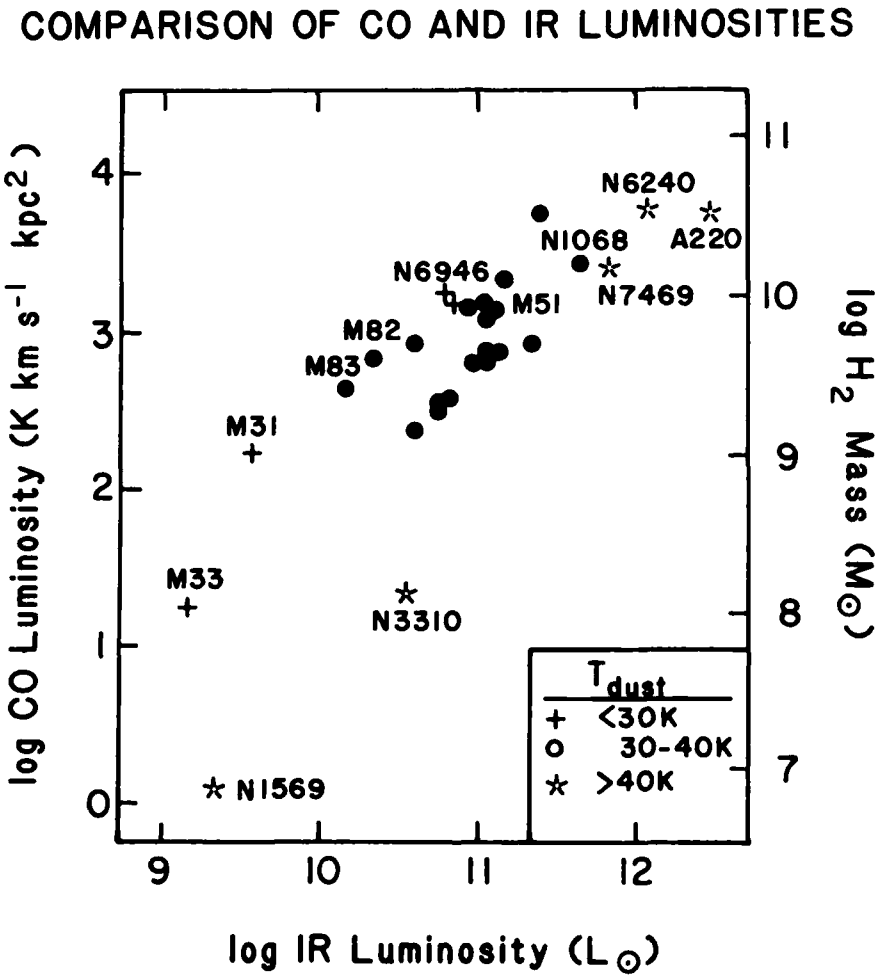

Fig. 19 — Comparison of the IRAS measured infrared (IR) luminosities with FCRAO measured total carbon monoxide (CO) luminosities for 28 galaxies. The positive correlation between the two quantities is clear. (From Young *et al.*, 1986.)

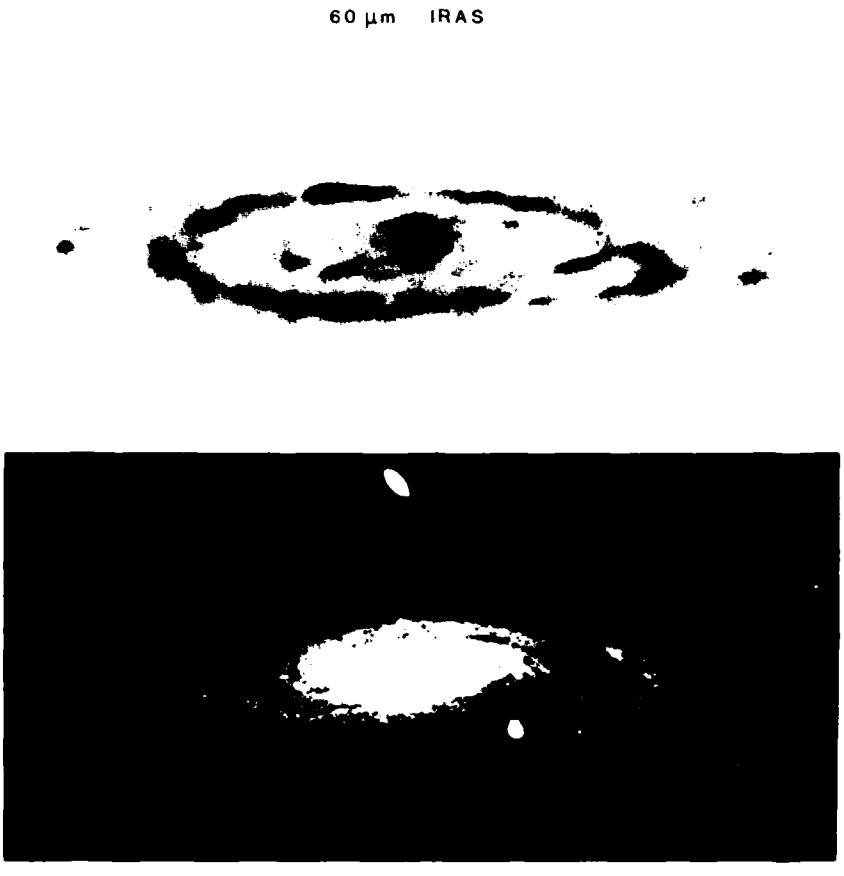

Fig. 20 — IRAS map of M31 at 60 μm (top) with the corresponding optical image (bottom). (From Habing *et al.*, 1984; p. L6 of "IRAS Observations of Radio-Quiet and Radio-Loud Quasars," by G. Neugebauer, published by the University of Chicago Press, copyright (c) 1984, used by permission.)


FILMED
58